Check for updates

Plasma Processes and Polymers

PLASMA PROCESSES AND POLYMERS

REVIEW OPEN ACCESS

Short Review on Plasma–Aerosol Interactions

Mario Janda[1] | Augusto Stancampiano[2] | Francesco di Natale[3] | Zdenko Machala[1]

[1]Department of Environmental Physics, Faculty of Mathematics, Physics and Informatics, Comenius University Bratislava, Bratislava, Slovakia | [2]GREMI UMR7344, CNRS-Université d'Orléans, Orléans, France | [3]Department of Chemical, Material and Industrial Production Engineering, University of Naples Federico II, Napoli, Italy

Correspondence: Zdenko Machala (machala@fmph.uniba.sk)

Received: 20 November 2024 | **Revised:** 6 December 2024 | **Accepted:** 8 December 2024

Funding: This study was funded by the EU NextGenerationEU through the Recovery and Resilience Plan for Slovakia under the project No. 09I03-03-V03-00033 EnvAdwice and ANR-23-CE04-0003 "PLASMASOL—Cold plasma and water aerosol: A new eco-friendly tool for agriculture", and is based upon collaboration within COST Action CA20114 PlasTHER, supported by COST (European Cooperation in Science and Technology).

Keywords: aerosol | charge effects | cold atmospheric plasma | droplets | plasma-activated aerosol | plasma–aerosol interactions | reactive oxygen and nitrogen species

ABSTRACT

Systems where cold atmospheric plasma interacts with liquid aerosols provide information on unexplored physico-chemical phenomena and yield multiple advantages. Plasma-activated aerosols show high chemical reactivity within small liquid microdroplet volumes, making them suitable for various applications and industrial processes. Plasma–aerosol interactions present complex interdisciplinary challenges that demand detailed investigations of the underlying physical, chemical, and transport mechanisms. This short review focuses on the key challenges in understanding plasma–aerosol interactions and the diagnostic hurdles in elucidating the physical and chemical mechanisms governing microdroplet interactions with plasma discharges. The scalability of plasma–aerosol systems, including high-throughput charged water flows, are analyzed. Some "niche" applications of plasma–aerosols are identified, especially in decontamination, nitrogen fixation, and agriculture. The controversies in the field are also introduced and critically discussed. The review concludes with a proposed path and outlook for the development of plasma–aerosol technology.

1 | Introduction

Aerosols, comprising tiny solid particles or liquid droplets suspended in gas, play significant roles in various environmental, health, and technological contexts. Examples such as dust, smoke, mist, and fog illustrate the diversity of aerosols, which can occur naturally or can be artificially generated. Their study is essential due to their profound impacts on climate change, air quality, and human health. Of particular concern is the role that aerosols play in transmitting infectious diseases [1]. Aerosols, especially those smaller than 5 μm in diameter, can carry pathogens such as viruses and bacteria, remaining airborne for extended periods. This characteristic facilitates the spread of respiratory diseases such as COVID-19, flu, and tuberculosis [2]. On the other hand, artificially generated aerosols are utilized in various industries, particularly in healthcare. Water aerosols, in particular, are used in medical inhalers to deliver medications directly into the lungs of patients suffering from respiratory conditions like asthma and chronic obstructive pulmonary disease [3]. Water aerosols are also integral to dust suppression systems in mining and construction industries, enhancing air quality and worker safety by minimizing particulate matter in the air [4]. Atomization of paint in spray and aerosols is a key technique for many industrial painting and coating processes. In agriculture, aerosols are a pivotal technology that enables efficient delivery of pesticides and herbicides. By dispersing chemicals as fine mists, farmers can apply them more accurately, reducing waste and thus the

This is an open access article under the terms of the Creative Commons Attribution-NonCommercial License, which permits use, distribution and reproduction in any medium, provided the original work is properly cited and is not used for commercial purposes.

© 2024 The Author(s). *Plasma Processes and Polymers* published by Wiley-VCH GmbH.

environmental impact [5]. However, despite these benefits, common chemical aerosols are still based on chemical agents that pose environmental risks, such as water contamination and adverse effects on beneficial insect populations. Thus, more sustainable aerosol technologies are needed to balance efficiency with environmental safety.

Plasma-treated or plasma-activated water (PAW) represents an innovative alternative to traditional chemical treatments, offering a more environmentally friendly approach. This technology uses cold atmospheric plasma (CAP), a state of matter in which energetic electrons exist alongside cooler, less energetic ions and neutral molecules. CAP generates reactive species like ions, radicals, and excited molecules, which can initiate chemical reactions at room temperature. Plasma can be generated by only using air and electrical power inputs. Plasmas in contact with water can generate reactive species such as nitrates NO_3^-, nitrites NO_2^-, hydroxyl radicals •OH, hydrogen peroxide H_2O_2, ozone O_3, and atomic oxygen •O, and thus constitute a nitrogen fixation technique or an advanced oxidation technique that may be free of solvent and long-term residuals and is therefore eco-friendly and sustainable. Most of the plasma reactor geometries that have been considered in the past decade consist essentially of batch processes where the plasma is generated either above the surface of the liquid or inside it. These configurations have demonstrated the potential of cold plasma in agriculture and medicine [6–8]. Nevertheless, various attempts to achieve technological transfer have highlighted the limitations in the scalability of these reactors, especially due to the limit in species transfer between the plasma phase (where they are produced) and the liquid phase (where they are stored or used).

Plasma-activated aerosols (PAAs), often referred to as plasma-activated mist (PAM) or fog, are a combination of cold plasma with micrometric aerosol particles (Figure 1). PAAs have the potential to overcome several limitations of classical batch configurations and offer special advantages in terms of controllability, thus providing new perspectives for plasma–liquid applications. The extremely high surface/volume ratio allows harvesting of ultrashort-lived reactive species that have a relatively small impact in batch processes due to their short depth of penetration. In fact, microdroplets can be regarded as microreactors that, through CAP action, can be chemically and physically tailored for specific effects and be easily delivered to the desired target. PAAs have also been reported to achieve extremely high yields of reactive species production [9] and pollutant degradation.

Plasma–aerosol interactions also show potential in medical applications. PAW aerosols have been proven to be effective in deactivating pathogens in aerosols, and surface decontamination, providing a more environmentally friendly solution to air and water purification [10–15]. This application is especially relevant in developing countries, where access to clean water and sanitation can be limited. Portable, low-energy plasma devices offer a practical way to decontaminate contaminated water or air, reducing the spread of infectious diseases and improving public health outcomes. Furthermore, PAAs have also been investigated for the removal of particulate matter, NO*x*, SO*x*, and volatile organic compounds (VOCs) from industrial and household exhaust gases [16–18].

In agriculture, PAAs show great promise in promoting crop growth while reducing the negative environmental impact typically associated with chemicals [19]. The use of PAA enables the creation of these reactive species with minimal energy input, making it an attractive technology for sustainable agriculture. Cold plasma has also been more recently investigated as a new source to generate charged aerosols for applications, such as rain enhancement [20].

Moreover, CAP can alter the chemical properties of aerosol surfaces, enabling applications in material synthesis, where aerosols serve as carriers or reactants in plasma-assisted

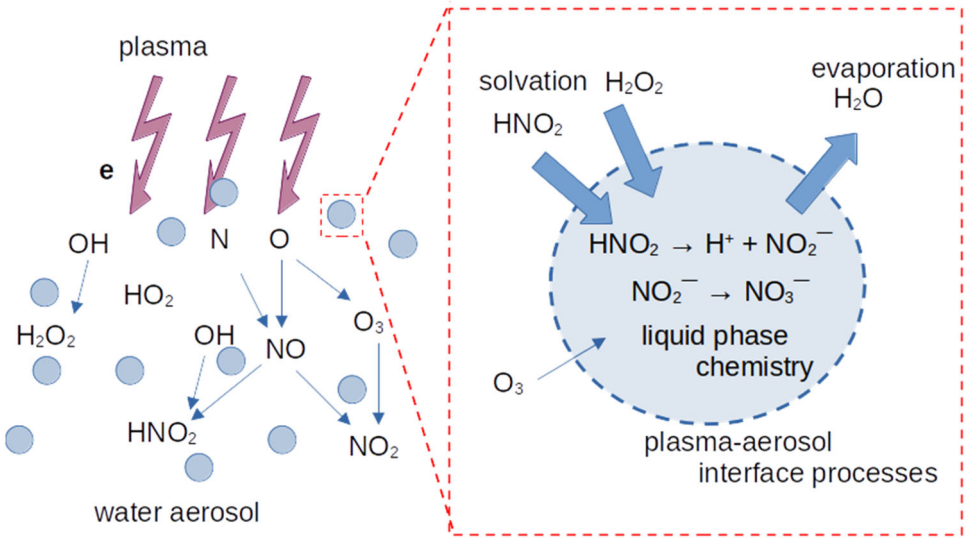

FIGURE 1 | Schematic representation of plasma–aerosol interactions, including the chemistry and transport of reactive oxygen and nitrogen species.

16128869, 0, Downloaded from https://onlinelibrary.wiley.com/doi/10.1002/ppap.202400275 by Mario Janda - Cochrane Slovakia , Wiley Online Library on [30/12/2024]. See the Terms and Conditions (https://onlinelibrary.wiley.com/terms-and-conditions) on Wiley Online Library for rules of use; OA articles are governed by the applicable Creative Commons License

processes such as plasma-assisted coating deposition of non-volatile precursors [21, 22]. The reactive species generated in the plasma (e.g., ions, radicals, excited molecules) can also interact with the solid aerosol particles, leading to chemical reactions. This can be used to modify the surface properties of particles or to synthesize new nanomaterials [23]. A range of new fascinating applications, such as the in-flight synthesis of nanoparticles for direct in situ delivery [24], can be envisaged thanks to PAA technology.

The number and variety of PAA system configurations are rapidly growing, but three common aerosol generator systems are usually adopted:

- *Pneumatic:* the water flow is fragmented into small droplets due to the friction with surrounding air. It may require an additional air flow (e.g., pressurized can, carburettors).
- *Piezoelectric:* a piezoelectric membrane presenting micrometric holes vibrates at high frequency and can produce fine aerosols (e.g., cosmetic moisturizers).
- *Electrospray:* the water flow is fragmented into small droplets by the effect of an electric field generated between a needle and a mesh or a ring.

These in turn can be combined with plasma generation systems, which usually include dielectric barrier discharges, plasma jets, corona, gliding arc, and transient spark (TS). The production of the aerosol mist usually takes place before its treatment by plasma, except for electrospray (ES), in which the same needle at high voltage can produce, at the same time and location, both the droplets and the plasma (e.g., TS discharge [13]). When a sufficiently high voltage is applied on the capillary (or nozzle) with a liquid flowing through it, the effective surface tension of the liquid starts to decrease due to the presence of an electric field, causing charge separation inside the liquid. This implies that the volume of the forming droplets decreases. When a critical voltage is reached, the shape of the droplet changes to conical, referred to as a Taylor cone [25]. Finally, a jet emerges from the tip of the Taylor cone and breaks into smaller droplets due to various instabilities [26, 27]. These charged droplets are then accelerated by the electric field: the ES phenomenon occurs. The droplets may further explode if their charge exceeds the Rayleigh limit [28, 29].

Whereas the numerous attractive applications mentioned above have led to research work, the theoretical and fundamental approach to this new category of plasma is lagging, and many of the underlying mechanisms remain barely investigated [30]. The generation of plasma in biphasic environments, where gas and liquid phases coexist, presents significant diagnostic and modeling difficulties. The behavior of charged aerosol droplets in plasma fields is influenced by factors such as droplet size, electric field strength, and plasma parameters [20]. Furthermore, plasma–aerosol interactions can introduce instabilities in plasma discharges, leading to inefficiencies. For example, aerosol particles can disrupt the plasma, causing streamer branching or premature discharge extinction. Understanding the fundamental mechanisms governing plasma–aerosol interactions is crucial to optimizing system performance and ensuring scalability for large-scale applications.

Thus, combining CAP with aerosol technology presents enormous potential for innovations in agriculture, environmental science, medicine, and industrial pollution control. PAAs offer efficient, sustainable alternatives to traditional chemical-based methods, reducing environmental impacts while enhancing process efficiencies. However, to fully realize the potential of plasma–aerosol systems, further research is needed to address the challenges of diagnostics, stability, and scale-up. Since 5 years ago, when a first opinion paper on plasma–aerosols was published, the number of papers published on the topic has significantly increased. In this review paper, we address the new emerging challenges, controversies, and perspectives in the field. By advancing our understanding of plasma–aerosol interactions, scientists can develop innovative solutions to some of the most pressing challenges of our time, from pollution and climate change to public health.

2 | Challenges in Understanding the Formation and Transport of Plasma-Reactive Species Into Aerosols

2.1 | Formation of Reactive Oxygen and Nitrogen Species (RONS) in CAP

The formation of RONS in cold atmospheric air plasmas is relatively well understood. Nonequilibrium plasmas in atmospheric air produce a complex mixture of gaseous RONS through numerous electron-driven and radical reactions [31]. Primary radical species such as hydroxyl radicals (•OH), atomic oxygen (O), and atomic nitrogen (N) are formed by the dissociation of air molecules (N_2, O_2, H_2O). These reactive species then recombine and interact with other radicals and molecules to form secondary RONS, including ozone (O_3), hydrogen peroxide (H_2O_2), nitrogen monoxide (NO), and nitrogen dioxide (NO_2^-) [32, 33].

The exact composition of these plasma-generated RONS is highly dependent on the specific plasma generation method used. Factors influencing this composition include the type of electrical discharge, power input to the plasma, and the gas composition.

For example, a corona discharge in dry air primarily produces ozone, whereas a dielectric barrier discharge could yield a broader range of species like ozone and nitrogen oxides, depending on the input power. Higher power generally leads to increased generation of reactive nitrogen species. It was found that low-power (0.04–0.1 W/cm^2) surface dielectric barrier discharge (SDBD) resulted in O_3 as the dominant species, whereas high-power (0.1–0.62 W/cm^2) SDBD resulted in the formation of nitrogen oxides [34]. In spark-like discharges (TS or gliding arc), the generation of nitrogen oxides dominates [35, 36].

When CAP is in contact with water (bulk or aerosol), the presence of water vapor significantly impacts the dominant

16128869, 0, Downloaded from https://onlinelibrary.wiley.com/doi/10.1002/ppap.202400275 by Mario Janda - Cochrane Slovakia , Wiley Online Library on [30/12/2024]. See the Terms and Conditions (https://onlinelibrary.wiley.com/terms-and-conditions) on Wiley Online Library for rules of use; OA articles are governed by the applicable Creative Commons License

RONS produced. Hydroxyl radicals (OH) are produced by reactions such as [37, 38] the following:

$$e + H_2O \rightarrow e + OH + H, \quad \text{(I)}$$

$$O\left(^1D\right) + H_2O \rightarrow OH + OH. \quad \text{(II)}$$

These OH radicals can significantly reduce O_3 through the following reactions [39]:

$$OH + O_3 \rightarrow HO_2 + O_2, \quad \text{(III)}$$

$$HO_2 + O_3 \rightarrow OH + 2O_2. \quad \text{(IV)}$$

Furthermore, OH radicals are crucial for the formation of hydrogen peroxide (H_2O_2) in the gas, for example, by the reaction (V) [40]:

$$OH + OH + M \rightarrow H_2O_2 + M. \quad \text{(V)}$$

The OH radical is also responsible for forming HNO_2 and HNO_3 through the reactions [33, 41]:

$$NO + OH + M\,(= O_2 \text{or } N_2) \rightarrow HNO_2 + M, \quad \text{(VI)}$$

$$NO_2 + OH + M \rightarrow HNO_3 + M. \quad \text{(VII)}$$

These reactions are also important in humid air without aerosols. However, the water content in humidified air is limited by the absolute partial water pressure at a given temperature, and in CAP, the gas temperature remains close to ambient temperature. In the case of plasma in contact with aerosols, the amount of water molecules in the gas phase can significantly increase under certain conditions.

In a TS discharge, the overall gas temperature remains close to ambient temperature, but TS generates thin spark plasma channels where the gas temperature temporarily increases above 2000 K [42]. In this confined hot gas region, a much higher absolute water vapor pressure can be obtained compared to the room temperature. This can explain the observed twofold increase of the relative Hα line intensity in the optical emission spectra of TS with ES microdroplets compared to the spectra of TS in humidified synthetic air [43]. The presence of the Hα line is mainly attributed to the impact of electrons on H_2O molecules [44]. Therefore, the increased Hα line intensity suggests that more H_2O molecules are dissociated into highly reactive H and OH radicals in TS with ES water microdroplets compared to TS in humidified gases.

The composition of the plasma gas influences the formation of aqueous RONS not only directly, by changing concentrations of gaseous RONS, but also indirectly. Different plasma gases lead to varying concentrations of dissolved gaseous species in the liquid, which can further impact RONS concentrations in the PAW [45]. For example, using O_2 plasma with dissolved O_2 in the water (without N_2) favors the formation of OH radicals compared to using air plasma, where both N_2 and O_2 are dissolved. Interestingly, the presence of only dissolved N_2 (without O_2) also promotes the formation of OH radicals (and nitrites and nitrates) compared to the case where both N_2 and O_2 are dissolved.

2.2 | Henry's Law on Solubility

In general, the solubility of the gaseous species in liquids, for example, water, is described by Henry's law solubility coefficient k_H:

$$k_H = c_i/p_i \quad (1)$$

where c_i is the molar concentration of i species in the aqueous phase and p_i is the partial pressure of that species in the gas phase [46]. The k_H is described as the proportionality factor of the amount of the dissolved gas in the aqueous phase to its partial pressure in the gas phase. In atmospheric chemistry, this coefficient is important to describe the distribution of trace species between the air and liquid droplets (aerosol). Henry's law coefficient can also be expressed as the dimensionless ratio between the aqueous-phase concentration c_i of i species and its gas-phase concentration c_g:

$$k_H{}^{cc} = c_i/c_g = k_H \times RT, \quad (2)$$

where R and T are the gas constant and temperature, respectively.

Henry's law coefficient, however, does not describe the rate of the solvation process. It relates concentrations in the gas and the liquid phase in steady state, with an equilibrated transfer (flux) of i species from the gas into the liquid phase, and the backward transfer (flux) from the liquid into the gas phase. Out-of-equilibrium steady state, which is typically the case in plasma–liquid interactions, these fluxes are not equal, assuming that kinetic equilibrium conditions with equal fluxes could lead to underestimation of the flux of the species entering the liquid [47]. Moreover, Henry's law does not take into account effects such as the geometry of the interface, the effect of an electric field (through polarization of the species), or the effect of electrical charges over the droplet that should be considered in plasma–aerosol interactions. Nevertheless, Henry's law solubility coefficient is a good indicator in the first approximation to assess which gaseous RONS should play important roles in the formation of aqueous RONS [48, 49].

The solubility of the gaseous RONS in water varies markedly, and even if their concentrations in the gas phase are similar, their achieved aqueous concentrations in water could be significantly different due to very different Henry's law solubility coefficients of each gaseous species [50]. Table 1 shows Henry's law solubility coefficients k_H (mol/m^3 Pa), including the dimensionless $k_H{}^{cc}$ constant, for the most typical long-lived gaseous plasma RONS [46].

The formation of RONS in aerosols in contact with plasma is influenced by several other factors, namely, the generation of reactive species in plasma, transfer of these species to aerosols, and chemical reactions inside the liquid phase.

16128869, 0, Downloaded from https://onlinelibrary.wiley.com/doi/10.1002/ppap.202400275 by Mario Janda - Cochrane Slovakia , Wiley Online Library on [30/12/2024]. See the Terms and Conditions (https://onlinelibrary.wiley.com/terms-and-conditions) on Wiley Online Library for rules of use; OA articles are governed by the applicable Creative Commons License

TABLE 1 | Henry's law solubility coefficients k_H and k_H^{cc} of gaseous species [46].

Gaseous species	k_H (mol/m^3 Pa)	k_H^{cc}
H_2O_2	9.1×10^2	2.26×10^6
HNO_2	4.8×10^{-1}	1.19×10^3
NO_2	1.2×10^{-4}	2.97×10^{-1}
NO	1.9×10^{-5}	4.71×10^{-2}
O_3	10^{-4}	2.48×10^{-1}
HNO_3	2.1×10^3	5.22×10^6

2.3 | Transport from the Gas Plasma to the Liquid

The transport of reactive species from the plasma gas, where they are generated, to the liquid, most typically water, is a complex process with many aspects that are not fully understood.

The interface between the plasma and water is a critical zone for the transport of reactive species. The properties of this interface, such as its surface area and charge, can affect the transport of reactive species. The lack of a clear definition of the interface (gas–liquid or plasma–liquid) is one of the challenges of the plasma–aerosol field. The interface is the boundary where the two phases (gas and liquid) meet. It is a very thin region, typically nanometers thick, where physical properties change dramatically. For example, the mass density decreases from around 0.9 g/cm^3 in the water droplet to almost zero within 0.5 nm [51]. The unique hydrogen-bonding network of water plays a crucial role in interfacial properties [52].

The interface is constantly in bidirectional fluxes, with water molecules evaporating into the gas and returning to the liquid. Evaporation from microdroplets is a more rapid process than the evaporation from a flat water surface. The curvature of the droplet plays a role, as molecules at the curved surface experience weaker intermolecular forces and can escape more easily. Evaporation from a flat surface is mainly influenced by factors like the temperature, the inlet gas flow rate, and its humidity. Droplet evaporation, however, is additionally affected by its size, shape, and velocity. However, the evaporation lifetime of microdroplets with a diameter as small as 10 μm is still relatively long (> 10 s even at 1000 K [53]), compared to the lifetime of many plasma-reactive species.

Reactive plasma species have different reactivities and lifetimes, which affect their transport to water. One of the main challenges in transporting reactive species to water is that they can be quickly quenched by reactions with other species in the gas phase or at the gas–liquid interface. This can reduce the number of reactive species that dissolve in the bulk water.

Species transport through the gas–liquid interface can be conceptualized by the change in density across the gas–liquid (plasma–liquid) interface. This transition occurs over a few nanometers or less. The rough interface has fluctuations with water exchanging from the bulk to the boundary over several picoseconds [54]. Water, which is considered as a model system in molecular dynamics simulations, provided an atomic-level insight into the plasma–liquid film interaction mechanisms. It was found that plasma-generated H_2O_2 molecules can travel through the water interface layer within 1.4 ns [51].

The plasma–liquid interface area is a key parameter that maximizes the contact between the plasma and the treated water solution, thus determining the obtained plasma chemical effects [55].

One of the ways to prepare the PAW efficiently is by improving the RONS transfer into water by increasing the total water surface area using the water aerosolization process by producing water microdroplets of a high surface-area-to-volume ratio [56]. This significantly increases the plasma–water interaction surface area and thus enables more efficient transfer of the plasma-reactive species into the water, which is of vital importance, especially for poorly soluble species, such as NO, NO_2, and O_3. Although aerosolization in some experimental arrangements reduced the RONS concentrations in PAW [57], the approach of increasing the plasma–liquid interaction surface area in microdroplets was adopted by several research groups [13, 58–63].

Despite the successful application of PAW formation by changing bulk water into the aerosol of microdroplets, the transport of reactive species from their generation in the plasma (gas phase) to water aerosols is a complex process that has not been fully understood as yet. Several approaches can be used to investigate this topic. One challenging approach involves using specialized diagnostic techniques to monitor species at the plasma–microdroplet interface.

Computational modeling can be used to simulate the transport of reactive species from CAP to liquids, especially water [56, 64–66]. This helps in identifying the factors that influence the transport and optimize plasma-based water treatment technologies. By using computational techniques, it was shown that a gas containing RONS generated by plasma in contact with water microdroplets is far from steady-state conditions assumed by Henry's law, where constant fluxes of species from the gas to liquid phase and back are assumed [56].

This can be demonstrated for the example of two species, hydrogen peroxide H_2O_2 and ozone O_3, because Henry's law solubility coefficient of H_2O_2 is almost seven orders of magnitude larger than that of O_3 (Table 1). This means that although H_2O_2 readily transfers into the water through the gas–liquid interface, O_3 is hardly dissolved into water due to its very low Henry's law coefficient. For this reason, the assumption of a constant partial pressure is generally valid only for weakly soluble species (with low k_H) species (e.g., O_3), as shown by Verlackt et al. [64], who investigated H_2O_2 and O_3 as examples of highly and poorly soluble cold plasma species in a 2D axisymmetric fluid model. The density of H_2O_2 shows a sudden decrease at the gas–liquid interface due to the fast transfer into the liquid, where its density is significantly higher compared to the gas phase. On the other hand, the density of O_3 remains constant above the gas-liquid interface for 1 min of plasma

16128869, 0, Downloaded from https://onlinelibrary.wiley.com/doi/10.1002/ppap.202400275 by Mario Janda - Cochrane Slovakia , Wiley Online Library on [30/12/2024]. See the Terms and Conditions (https://onlinelibrary.wiley.com/terms-and-conditions) on Wiley Online Library for rules of use; OA articles are governed by the applicable Creative Commons License

treatment, where its density is much higher in the gas phase compared to the liquid phase. For highly soluble species (e.g., H_2O_2), the gas density of species is not significantly depleted and can be considered constant only if the total volume of water is small and thus a small amount of the gas-phase species can be dissolved. Kruszelnicki et al. calculated that for aerosol solvation, the H_2O_2 depletion is negligible only for microdroplets with a diameter below ~30 μm [56]. For bigger microdroplets with a larger volume, the surrounding H_2O_2 of these microdroplets was already depleted.

Further insights can be gained by systematically correlating the composition of RONS in both gas and liquid phases under various experimental conditions (different plasma sources, power, gas composition). There are relatively few studies that sufficiently address the composition of both gaseous and liquid products in the formation of PAW [67]. However, computational models require validation by reliable experimental data, which are still very limited.

Typical long-lived plasma oxidizing species, H_2O_2, and its formation in multiple plasma–water systems have been extensively studied over the last few decades. In a review by Locke et al., the formation of H_2O_2 was investigated in various plasma reactors with discharges directly in and over the liquid water with bubbles, and capillary discharges, in terms of H_2O_2 gas–liquid mass transfer characteristics. The highest H_2O_2 yields were found for the water droplet spray, which provides large surface areas and small length scales to enhance the mass transfer rates [9].

Gorbanev et al. [68] and Winter et al. [69] assessed the transition of H_2O_2 into the liquid and found a direct correlation between the concentration of H_2O_2 in the gas phase and the liquid media.

With increasing H_2O_2 amount in the gas phase, the aqueous H_2O_2 concentration increased, irrespective of whether H_2O_2 was created by the plasma in the gas phase or by the H_2O_2 bubbler (without plasma), with a slightly higher liquid H_2O_2 concentration for the plasma case [69].

Machala et al. [70] observed the formation of RONS by two types of atmospheric air plasma discharges in contact with water: streamer corona (SC) and TS. SC discharge was characterized by low power (0.2–0.4 W), short low current pulses (~10 mA, 10–100 ns), and a typical repetition frequency of 10–30 kHz, whereas TS was characterized by higher power (1.5–2.3 W), short high current pulses (~10 A, ~25 ns), and a typical repetition frequency of 1–4 kHz [71]. Use of SC predominantly yielded the formation of H_2O_2 and O_3, and use of TS yielded H_2O_2 and (H)NO*x*. The produced gaseous RONS are readily dissolved in water, resulting in aqueous $H_2O_{2(aq)}$, $O_{3(aq)}$, NO_2^-, and NO_3^-, respectively, in the PAW.

Additionally, simplified experiments focusing on the transport of single species from an external source (e.g., pressure cylinders) to water aerosols can enhance our understanding of RONS solvation to water aerosol. In this context, comparison of the transport of RONS to bulk water with that to aerosols is also crucial.

Hassan et al. recently studied the transport mechanism of medium versus weakly soluble gaseous RNS, namely, HNO_2, NO_2, and NO generated in atmospheric air external sources in contact with bulk water, and two different aerosol interaction systems using either nebulized or ES microdroplets [49]. This work follows a previously published work in which the transport mechanism of highly and poorly soluble ROS (H_2O_2 and O_3) in bulk water and electrosprayed microdroplets (depicted in Figure 2) was studied [48].

The solvation rate of H_2O_2 and O_3 increased with the treatment time and the gas–liquid interface area. The total surface area of the electrosprayed microdroplets was much larger than that of the bulk, but their lifetime was much shorter. It was estimated that only microdroplets with diameters below ~40 μm could achieve saturation by O_3 during their lifetime. This finding aligns with computational results [56], where the $O_{3(aq)}$ density reaches saturation during the simulation after 1 ms of O_3 solvation from the plasma, regardless of the droplet diameter (5–20 μm). Notably, O_3 saturation was also observed in experiments with bulk water with a flat surface, although a longer treatment time was required. For example, with 450 ppm of O_3 in air at a flow rate of 1.6 slm and a bulk water surface area of 13 mm^2, 0.2 nmol of O_3 dissolved after 1 min, whereas only 0.5 nmol dissolved after 4 min, which indicates nonlinear solvation, hence the saturation effect [48].

For bigger ES microdroplets where the saturation is not achieved during their (flying) lifetime, the solvation of O_3 can continue even after the microdroplets reach the reactor walls. On the other hand, the saturation by H_2O_2 in the ES microdroplets was unreachable due to its depletion from air [48]. The solvation of H_2O_2 thus continued after the flying period of microdroplets. Besides the short-lived flying ES microdroplets, the longer-lived microdroplets deposited on the reactor bottom/walls therefore substantially contributed to the solvation of H_2O_2 and > 40 μm microdroplets even of O_3 [48].

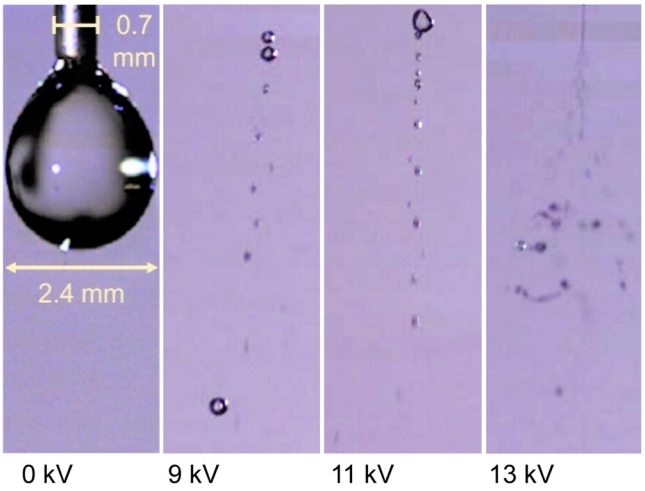

FIGURE 2 | High-speed camera imaging of water electrospray at various voltages, 300 μL/min. Data from the experiments of M.E. Hassan, M. Janda, and Z. Machala and in part reprinted from [48] with permissions.

16128869, 0, Downloaded from https://onlinelibrary.wiley.com/doi/10.1002/ppap.202400275 by Mario Janda - Cochrane Slovakia , Wiley Online Library on [30/12/2024]. See the Terms and Conditions (https://onlinelibrary.wiley.com/terms-and-conditions) on Wiley Online Library for rules of use; OA articles are governed by the applicable Creative Commons License

It was confirmed that among NO, NO_2, and HNO_2, the latter is the dominant contributor to NO_2^- ion formation in water [49]. A higher transport efficiency of O_3 and a much higher NO_2^- formation efficiency from gaseous NO_2 or HNO_2 than predicted by Henry's law were observed compared to the transport efficiency of H_2O_2, which corresponds to the expected Henry's law solvation. This could be attributed to the depletion of the H_2O_2 concentration in the g⁻as phase, as predicted by computational simulations.

The improvement of the transport/formation efficiencies by nebulized and ES microdroplets, where the surface area is significantly enhanced compared to the bulk water, is most evident for the solvation enhancement of the weakly soluble O_3 [49]. NO_2^- ion formation efficiency was strongly improved in ES microdroplets with respect to bulk water and even nebulized microdroplets, which is likely due to the charge effect that enhanced the formation of aqueous nitrite NO_2^- ions when NO_2 or HNO_2^- are transported into water (shown in Figure 3).

With simplified experiments using external sources of RONS, it is only possible to study the solvation of long-lived species to aerosols. The influence of short-lived species on the formation of RONS in the liquid phase can be determined from experiments where the production of liquid-phase RONS by direct contact with plasma is compared to the production of RONS when aerosols are in contact with gas previously treated by electrical discharges. In the first case, formation of aqueous RONS can be influenced both by short-lived and by long-lived species. Without direct contact of water aerosols with plasma, only long-lived species can be solvated.

Pareek et al. recently studied the generation of PAW by TS discharge in different gases (N_2, O_2, and synthetic air, dry or humidified) with direct or indirect contact of the discharge with water aerosol formed by the ES process [43]. In direct contact,

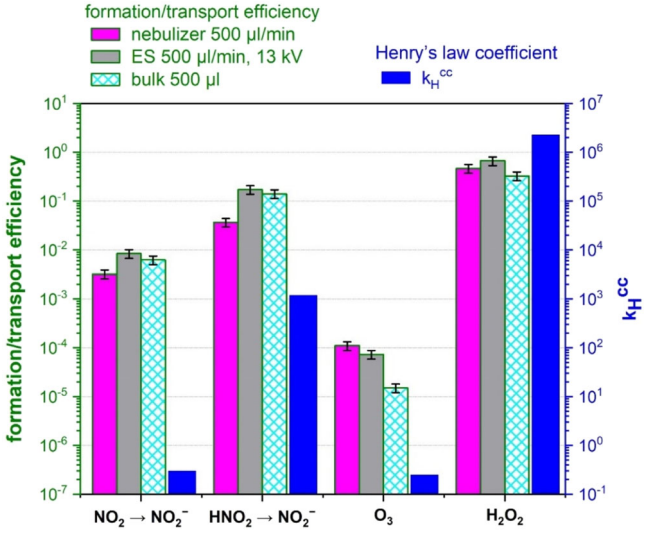

FIGURE 3 | Comparison of the formation efficiency of NO_2^- from NO_2 and from HNO_2, and the transport efficiency of O_3 and H_2O_2 in nebulized and electrosprayed (ES) microdroplets, and bulk water, shown with dimensionless Henry's law coefficients (k_H^{cc}). Reprinted from [49], with permissions from Springer Nature to open access publications.

ES aerosol was generated within the discharge zone. In the indirect treatment, the gas was first treated by the TS discharge and sprayed by the water aerosol in the second section of the reactor. It was found that in the case of TS discharge, $H_2O_{2(aq)}$ in water is mainly formed due to short-lived reactive species, such as OH radicals, and not by dissolution of gaseous H_2O_2.

2.4 | Chemical Reactions in the Liquid Water

Some aqueous RONS, such as H_2O_2 and O_3, can be transported from the plasma phase to the water without chemical conversions. However, other aqueous-phase RONS are formed through chemical reactions within the liquid phase. For example, aqueous hydrogen peroxide ($H_2O_{2(aq)}$) can be produced by the direct solvation of OH radicals transported into the water, where they undergo a two-body reaction [72, 73]:

$$OH_{(aq)} + OH_{(aq)} \rightarrow H_2O_{2(aq)}. \quad \text{(VIII)}$$

As OH radicals are highly reactive and can be easily quenched in the gas phase (e.g., by reactions III, V–VII), this pathway is primarily possible only with direct contact between the water aerosol and the plasma. More generally, direct plasma treatment refers to a setup where the target (in this case, the aerosol droplets) is partially or fully inside the plasma phase. In a direct configuration, the aerosol droplets are immersed in the plasma phase and subjected to interactions with free electrons, ions, and short-lived reactive species (e.g., OH radicals). Conversely, in an indirect configuration, the aerosol droplets remain in the gas phase (typically air) and interact only with long-lived reactive species (e.g., H_2O_2), which can diffuse from the plasma through the gas to the liquid surface.

It is likely that other short-lived species also play a significant role in the formation of $H_2O_{2(aq)}$ when direct contact between water aerosol and plasma occurs. $H_2O_{2(aq)}$ can also be formed through liquid-phase reactions involving dissolved HO_2 radicals [9, 74]:

$$HO_{2(aq)} + HO_{2(aq)} \rightarrow H_2O_{2(aq)} + O_2, \quad \text{(IX)}$$

or by a sequence of electron (e) and proton (H^+) associative reactions (X and XI):

$$HO_{2(aq)} + e_{(aq)} \rightarrow HO_{2(aq)}^-, \quad \text{(X)}$$

$$HO_{2(aq)}^- + H_{(aq)}^+ \rightarrow H_2O_{2(aq)}. \quad \text{(XI)}$$

Interaction of dissolved singlet atomic oxygen ($O(^1D)$) with H_2O molecules has also been reported to result in the formation of $H_2O_{2(aq)}$ [75, 76]:

$$O\left(^1D\right)_{(aq)} + H_2O \rightarrow H_2O_{2(aq)}. \quad \text{(XII)}$$

Nitrates (NO_3^-) and nitrites (NO_2^-) can be produced by the direct solvation of nitric acid (HNO_3) and nitrous acid (HNO_2) molecules, followed by their dissociation in liquid water:

16128868, 0, Downloaded from https://onlinelibrary.wiley.com/doi/10.1002/ppap.202400275 by Mario Janda - Cochrane Slovakia , Wiley Online Library on [30/12/2024]. See the Terms and Conditions (https://onlinelibrary.wiley.com/terms-and-conditions) on Wiley Online Library for rules of use; OA articles are governed by the applicable Creative Commons License

$$HNO_{3(g)} \rightarrow HNO_{3(aq)} \leftrightarrow H^+_{(aq)} + NO^-_{3(aq)}, \quad \text{(XIII)}$$

$$HNO_{2(g)} \rightarrow HNO_{2(aq)} \leftrightarrow H^+_{(aq)} + NO^-_{2(aq)}. \quad \text{(XIV)}$$

Alternative pathways for NO_3^- and NO_2^- formation involve the solvation of NO, NO_2, and N_2O_5 to $NO_{(aq)}$, $NO_{2(aq)}$, $NO_{3(aq)}$, and $N_2O_{5(aq)}$, respectively [77]:

$$NO_{(aq)} + NO_{2(aq)} + H_2O \rightarrow 2\,NO^-_{2(aq)} + 2H^+, \quad \text{(XV)}$$

$$NO_{2(aq)} + NO_{2(aq)} + H_2O \rightarrow NO^-_{2(aq)} + NO^-_{3(aq)} + 2H^+_{(aq)}, \quad \text{(XVI)}$$

$$NO_{3(aq)} + H_2O \rightarrow OH_{(aq)} + NO^-_{3(aq)} + H^+_{(aq)}, \quad \text{(XVII)}$$

$$N_2O_{5(aq)} + H_2O \rightarrow 2NO^-_{3(aq)} + 2H^+. \quad \text{(XVIII)}$$

However, if HNO_2^- is present in the gas phase, it becomes the dominant source of NO_2^-, even if the concentrations of NO and NO_2 in the gas are higher [49, 78]. Very likely, the same can also be claimed about HNO_3 with respect to the other possible sources of $NO_3^-{}_{(aq)}$, such as gaseous N_2O_5 and NO_3. Based on Henry's law constant (Table 1), HNO_3 has much better solubility than even HNO_2, and the concentrations of N_2O_5 or NO_3 in the gas would have to be higher than the HNO_3 concentration by several orders of magnitude to have a dominant effect on $NO_3^-{}_{(aq)}$ formation. Further research is still needed to resolve this issue.

Depending on the plasma source properties, or treatment time, the resulting NO_2^-/NO_3^- ratio in freshly produced PAW can vary significantly [43, 70, 79].

Afterward, the NO_2^-/NO_3^- ratio undergoes further changes, especially if the PAW has a low pH or contains a significant amount of $H_2O_{2(aq)}$.

The acidification of PAW results from the production of $H^+{}_{(aq)}$ by reactions (XIII to XVII). At low pH, $NO_3^-{}_{(aq)}$ is also formed from $NO_2^-{}_{(aq)}$ by a disproportionation reaction [80]:

$$3\,NO^-_{2(aq)} + 3H^+ \rightarrow 2NO_{(aq)} + NO^-_{3(aq)} + H^+ + H_2O. \quad \text{(XIX)}$$

If the initial PAW pH is not too low, the decrease in the $NO_2^-{}_{(aq)}$ concentration is relatively slow. Pareek et al. observed an exponential-like decrease in the $NO_2^-{}_{(aq)}$ concentration with a characteristic time constant of 2200 min, even at an initial pH of about 3.4 [43]. In the presence of $H_2O_{2(aq)}$ at an initial concentration roughly equal to the initial concentration of $NO_2^-{}_{(aq)}$, the concentration of both species decreased much faster, with a characteristic decay time of about 40 min. This is because, under acidic conditions, $NO_2^-{}_{(aq)}$ can react with $H_2O_{2(aq)}$ through the following reactions [79–81]:

$$NO^-_{2(aq)} + H_2O_{2(aq)} \rightarrow NO^-_{3(aq)} + H_2O, \quad \text{(XX)}$$

$$NO^-_{2(aq)} + H^+_{(aq)} + H_2O_{2(aq)} \rightarrow ONOOH_{(aq)} + H_2O, \quad \text{(XXI)}$$

$$NO^-_{2(aq)} + H^+_{(aq)} + 2\,H_2O_{2(aq)} \rightarrow O_2NOOH_{(aq)} + 2H_2O. \quad \text{(XXII)}$$

These reactions are responsible for the aging of PAW. On the other hand, they demonstrate that for the production of peroxynitrous acid ($ONOOH_{(aq)}$) and peroxynitric acid ($O_2NOOH_{(aq)}$), which play an important role in the antimicrobial effects of PAW [82], it is beneficial to generate a mixture of $H_2O_{2(aq)}$ and $NO_2^-{}_{(aq)}$ in the liquid phase. If the PAW generation time is too long, the final composition of PAW is significantly influenced by these reactions, and the major final long-lived species to be expected is $NO_3^-{}_{(aq)}$.

The pH and initial dissolved organic matter content of the water solution can affect the concentration of reactive species in PAW. For example, •OH radicals can be scavenged by dissolved organic matter, and NO_2^- can be converted into NO_3^- at low pH. The presence of specific biomolecules in the cell culture media, like the amino acid L-tyrosine, effectively creates alternative routes of RONS formation, which cannot be related only to the action of the plasma [83, 84].

3 | Diagnostics Challenges

Diagnostics of aerosol microdroplets imposes numerous challenges due to their inherent characteristics. Their small size pushes the limits of optical diagnostic techniques for their detection. The chaotic motion of these droplets, driven by Brownian motion and air currents, makes it difficult to track and analyze individual particles. Their relatively short lifetime, influenced by evaporation, condensation, and coagulation, further complicates real-time analysis. Despite these challenges, several techniques are available for droplet analysis that provide information about the size and amount (concentration) of aerosol microdroplets. Nevertheless, developing noninvasive techniques for diagnosing aerosol microdroplets' chemical composition or for diagnosing surface processes remains a significant challenge.

3.1 | Droplet Size/Amount Determination

The size of charged microdroplets generated by ES can be estimated from the measured electric current corresponding to their carried electric charge [85]. However, for an accurate estimate of droplet size, it is necessary to distinguish between the discharge current and the current carried by charged ES microdroplets. It is possible to separate these two currents in the case of continuous glow corona discharge [86]. However, it becomes much more complicated in pulsed discharges.

Imaging techniques are also frequently used to monitor microdroplets [87–89]. Modern fast cameras enable recording of videos with a high frame rate for microdroplet visualization and enable obtaining droplet size from camera photographs. However, the process is quite laborious and requires detailed post-processing of the obtained photographs.

Several other techniques are available for droplet size/concentration diagnostics. These include imaging techniques based on

16128869, 0, Downloaded from https://onlinelibrary.wiley.com/doi/10.1002/ppap.202400275 by Mario Janda - Cochrane Slovakia , Wiley Online Library on [30/12/2024]. See the Terms and Conditions (https://onlinelibrary.wiley.com/terms-and-conditions) on Wiley Online Library for rules of use; OA articles are governed by the applicable Creative Commons License

shadowgraphs and holography, diffractometry, particle-sizing interferometry, and optical counters based on light scattering (see [90] and references therein). Based on these techniques, several probes were developed, useful, for example, for wet steam investigation in power plants [91, 92]. However, these probes as well as some of the methods are not suitable for droplets' characterization in small gaps used to generate ES with the discharge. For the ES characterization, several authors also used phase Doppler anemometry [93, 94]. This technique allows measurement of the size distribution and velocity of droplets, as well as their concentration. The measurement point is determined by the intersection of two focused laser beams. As a particle moves through the measurement point, it scatters light from both laser beams, generating an optical interference pattern. The light-collecting optics projects a fraction of the scattered light onto multiple detectors. Each detector converts the optical signal into a Doppler burst with a frequency linearly proportional to the particle velocity. The phase shift between the Doppler signals from different detectors is a direct measure of the particle diameter.

Laser scattering techniques like Mie scattering and dynamic light scattering (DLS) are used to measure the size distribution and concentration of aerosol particles. Use of these methods can enable determination of how the plasma affects the particle size, morphology, and agglomeration [95]. Recently, a relatively simple technique suitable for the detection of larger charged microdroplets (diameter of 10–400 μm) combining electrical current measurement and attenuation of light intensity of two planar laser beams was developed [96].

3.2 | Ex Situ Chemical Diagnostics of PAW

The concept of transforming bulk water into aerosol microdroplets centers on increasing the surface area to volume ratio. This enhancement facilitates the transport of reactive species from the gas phase to the liquid phase. To study this transport indirectly, the composition of condensed aerosol that has been exposed to a gas-containing reactive species can be analyzed. This ex situ diagnostic provides valuable information about the extent of species transfer and the nature of the chemical transformations that occur within the aerosol droplets.

However, this indirect ex situ method is best performed in single-species experiments to avoid interference between various gas-phase RONS and the formation of liquid-phase products, for example, NO_2^- by solvation of different gas-phase species [49]. Another drawback of this indirect ex situ approach is the relatively long time needed to accumulate enough condensed aerosol microdroplets for analysis. During this time, partial conversion of solvated RONS can occur, for example, by a disproportionation reaction that involves conversion of NO_2^- into NO_3^- at lower pH [80].

3.3 | In Situ Aerosol and Interface Diagnostics

Results from specialized diagnostic techniques to monitor species in situ in aerosol microdroplets or at the plasma–microdroplet interface are therefore highly valuable. Several challenging approaches can be used to research this topic. One challenging approach involves using specialized diagnostic techniques to monitor species at the plasma–microdroplet interface. Sremacki et al. [57] studied the role of aqueous aerosols in modulating reactive species production by an RF plasma jet. A combination of several physical and chemical analytic techniques was used. Optical emission spectroscopy, electron paramagnetic resonance spectroscopy, and a biochemical model based on cysteine as a tracer molecule have been applied. This research revealed that aerosol injection shifts the production of ROS from atomic and singlet oxygen toward OH radicals, which are generated in the droplets. Species generation occurred mainly at the droplet boundary layer during their transport through the effluent.

Oinuma et al. [59] studied the transport of OH generated by an RF plasma to controlled-size microdroplets containing formate. Detailed plasma diagnostics, ex situ analysis of the plasma-induced chemistry in the droplet, droplet trajectory, and size measurements enabled a quantitative study of the reactivity transfer of OH from the gas-phase plasma to the liquid phase. The key point of their success was a controlled plasma–droplet interaction experiment, with stable plasma and controlled formation of single-sized microdroplets by a micro-droplet dispenser, with a specified plasma–microdroplet interaction time. The obtained results enabled validation of a one-dimensional reaction–diffusion model used to calculate the OH transport and formate oxidation inside the droplet. The model showed that formate conversion is dominated by near-interfacial reactions with OH radicals and is limited by the diffusion of formate in the droplet.

In situ monitoring of the plasma–liquid interface is also possible by using Raman light sheet microspectroscopy [97]. The Raman modes of the −O−O stretch of H_2O_2 and the symmetric stretch of NO_3^- and −OH bend of water can be measured simultaneously while measuring at depths less than about 20 μm from the interface. Recently, it was shown that this technique can also be used to monitor NO_3^- in ES microdroplets [98]. However, the detection limit needs to be improved from about 1 mM to much lower values, so that this technique can be used for probing the gradual increase of NO_3^- in the microdroplets exposed to the plasma. This could probably be achieved by using the coherent anti-Stokes Raman scattering technique.

3.4 | Single-Droplet Diagnostics

Aerosol production is inherently chaotic, particularly regarding the spatial distribution of droplets. This variability poses significant challenges for performing repetitive measurements with micrometric spatial resolution. Achievement of a reproducible aerosol droplet distribution remains an unresolved issue, even within the broader field of aerosol science. To tackle the complexity of plasma–aerosol multiphase and multiscale systems, a few groups attempted to investigate the interaction of plasma discharges with a single water droplet. Maguire et al. successfully conducted a study in which controlled single-microdroplet streams were exposed to an RF plasma with optical imaging, which opens up possibilities for gas-phase

16128869, 0, Downloaded from https://onlinelibrary.wiley.com/doi/10.1002/ppap.202400275 by Mario Janda - Cochrane Slovakia , Wiley Online Library on [30/12/2024]. See the Terms and Conditions (https://onlinelibrary.wiley.com/terms-and-conditions) on Wiley Online Library for rules of use; OA articles are governed by the applicable Creative Commons License

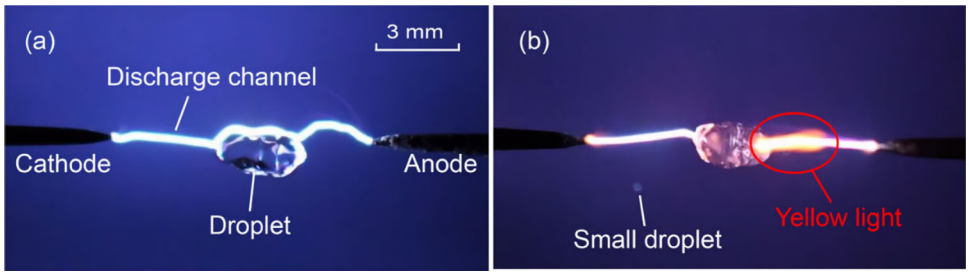

FIGURE 4 | Discharge digital photos of suspended droplets with different conductivities in a needle–needle electrode. (a) Low-conductivity droplet. (b) High-conductivity droplet. Reprinted from [101], with permissions from John Wiley & Sons.

microreactors and remote delivery of active species for plasma medicine [99]. Another approach, also derived from the aerosol scientific domain, is to initiate the suspension of a single droplet ether by a capillary [100] or through acoustic levitation [101], exposed to a pin-to-pin nanosecond discharge. These studies offer useful insight into the propagation of the plasma discharge in the presence of a relatively big water droplet (a few millimeters) of high conductivity (2–50 mS/cm) and are in partial agreement with the computational work performed by Babaeva et al. on streamer propagation in the presence of micrometric particles [102]. In these studies, the plasma propagates from the high-voltage electrode to the droplet and reignites on the opposite side of the droplet to propagate toward the ground electrode. This phenomenon is not observed in the case of low-conductivity droplets (< 0.5 mS/cm), for which the plasma appears to propagate around the droplet surface (Figure 4). Thus, liquid conductivity as well as its permittivity appear to be pivotal parameters that determine plasma propagation in the presence of droplets.

It should be noted that during plasma–aerosol interactions, RONS are being delivered into the droplets, including transport and formation ions (e.g., NO_2^-) imposing charges therein, which increases the liquid conductivity during this treatment. Consequently, the low-conductivity droplet behavior where plasma propagates around the (dielectric) droplets may transform into high-conductivity behavior where (conductive) droplets are bridging the discharge propagation. This phenomenon is more likely to occur with microdroplets of smaller sizes with higher surface-to-volume ratios, thus enhanced RONS transport. To the authors' knowledge, this has not been experimentally investigated in the literature.

4 | Identifying the "Niche" Applications

Identifying the "niche" applications of PAAs represents a challenge for this novel technology in the broad field of established aerosol applications. The type of application is typically driven by the chemical composition of PAW/PAA and its effect. A major advantage of PAA with respect to more commonly used PAW applications is that when PAW is aerosolized, only small amounts are sufficient, as opposed to large volumes, for example, in agriculture applications. Compared to applying bulk liquid PAW, PAA are very chemically efficient, especially because they represent micro-reactors due to the very efficient transfer of plasma-reactive species into microdroplets.

4.1 | Antimicrobial and Therapeutic Effects of PAA

The most investigated applications of PAA (often called plasma-activated mist, PAM) are based on its potent antimicrobial properties. They stem from reactive species such as H_2O_2, O_3, NO_2^-, and in some cases, even transient $ONOO^-$, O_2^-, and $^1O_2$ delivered into the aerosol microdroplets during plasma activation. PAAs were used, for example, in inactivating pathogenic bacteria [14, 103, 104]. During the COVID-19 pandemic, several novel approaches using PAAs in combating the aerial spread of pathogens, including surrogate viruses for coronavirus, were published [15, 105, 106]. PAAs were also tested for disinfecting virus-laden objects such as respirators [107] or hard surfaces [11, 108]. A general review of the non-thermal plasma inactivation of coronavirus, including plasma–aerosol treatments, was carried out by Han et al. [109].

Another area of applications where PAA or plasma enhancement of disinfectant-containing aerosols, for example, solutions of H_2O_2 [110], can be very conveniently applied, is the treatment of various fresh produce (e.g., lettuce, spinach, kale, various fruits) and food products (e.g., beef), leading to disinfection and extension of their shelf-life [111–113]. PAAs also have emerging applications in medicine, especially in the treatment of respiratory tract infections [106] or even in developing novel cancer treatments [114].

4.2 | Nitrogen Fixation and Agriculture

Nitrogen fixation is one of the key chemical engineering processes, leading mostly to the production of ammonia (NH_3), which is an essential building block for fertilizers, chemicals, and energy carriers. Nitrogen fixation supports diverse biological, agricultural, and industrial processes, especially in producing synthetic fertilizers. Typically performed by the Haber–Bosch process in large-scale industrial plants at high pressure and temperature, it is currently one of the leading producers of carbon emissions at a global scale. Novel solutions to decarbonize nitrogen fixation include plasma-electrified synthesis of NH_3, as well as other forms of nitrogen (e.g., nitrites and nitrates), using water and atmospheric nitrogen. The intrinsic limitations of the state-of-the-art plasma-based nitrogen fixation solutions include energy efficiency; scalability; direct use of clean renewable energy; and direct sustainable application of water-based nitrogen fixation [19]. It has been

16128869, 0, Downloaded from https://onlinelibrary.wiley.com/doi/10.1002/ppap.202400275 by Mario Janda - Cochrane Slovakia , Wiley Online Library on [30/12/2024]. See the Terms and Conditions (https://onlinelibrary.wiley.com/terms-and-conditions) on Wiley Online Library for rules of use; OA articles are governed by the applicable Creative Commons License

shown that nitrogen gas and water droplets, that is, aerosol, can serve as feeds in a plasma process for the sustainable and distributed production of ammonia or other fixed nitrogen compounds, such as nitrates and nitrites [115].

PAA (plasma-activated aerosol/mist) has interesting applications in aeroponic plant cultivation. PAA nitrogen fixation systems are applied for the continuous delivery of nitrogen-based nutrients directly to the roots of living plants using a custom-designed aeroponic system that increases the leaf emergence rate and leaf area of bean sprouts by more than 30% [19]. In parallel to fixed nitrogen, PAAs contain reactive species promoting germination and plant growth.

A few research groups demonstrated the advantages of direct air plasma- and indirect PAM on germination, and physiological parameters of rice seeds [116] and growth parameters of maize plants [117]. The recent review and roadmap paper of Bilea et al. [6] introduced the topic of plasma agriculture by describing in detail various plasma sources with potential for agricultural applications, as well as the effects of plasma exposure of seeds, both at the macroscopic scale, and concerning the intricate mechanisms occurring within plants. Generally, the main plasma-induced effects for all types of seeds include increased germination, higher plant yield, seed decontamination, and sometimes higher tolerance to various stress factors. These effects are due to the physical and chemical plasma interaction with seeds, followed by the response of cell mechanisms.

4.3 | Other Applications

Water sprays and aerosols are very efficient methods to increase air/gas humidity. The introduction of water droplets in the plasma region will greatly increase the water vapor content in the gas. It is known that high water content (70%–80% RH) in the plasma region can lead to an increase in the production of species such O_3 and H_2O_2 [118, 119] and generally to higher decontamination efficiency [120]. On the other hand, completely H_2O-saturated gases (with 100% RH) were also associated with less uniform plasma discharges and lower decontamination efficacy [121]. The literature on the propagation of plasma discharges in gas mixtures with high water vapor is still sparse and limited. A better understanding of the water vapor gradient in plasma–aerosol systems and plasma propagation in humid gases would greatly promote the advancement of this technology.

Another unique application is the use of PAW aerosolized spray cooling, introduced by Low et al., as an effective method for rapidly absorbing excess heat from high-temperature surfaces, such as light-emitting diodes. Compared to deionized aerosols, PAAs have lower surface tension, which facilitates rapid evaporation when deposited on a heated surface. When applied to the cooling of LED bulbs, this technique increases the heat transfer coefficient by up to 45%, leading to a 30% increase in illuminance. Importantly, this approach does not require modifications to the existing spray cooling systems, such as those involving surface coatings [122].

5 | Up-Scaling of Plasma–Aerosol Systems

In the largest majority of existing applications, ES systems are operated in cone jet mode for the stable production of nearly monodisperse microdroplets. Cone jet mode refers to a stable operating regime in which a liquid, typically delivered through a fine capillary, is subjected to a high electric field, causing the liquid at the capillary tip to deform into a conical shape (Taylor cone). From the apex of this cone, a fine jet of liquid is emitted, which subsequently breaks up into highly charged microdroplets due to electrostatic forces. Such ESs typically operate at very low flow rates, from μL/h to mL/h.

Nowadays, larger flow rate electrospraying is proficiently used in agriculture and industry because of the interesting features of charged sprays. For example, PAA (PAM) applications in aeroponic plant cultivation are based on the continuous, scalable, in-flow generation of PAA containing NH_4^+, NO_3^-, NO_2^-, and other nitrogen fixation species through the reaction of air plasma and high-flux water mist containing large area-to-volume ratio micron-sized droplets. Through the solar-energy-driven plasma-assisted oxidation confined within the droplet micro-reactors, a liquid-phase nitrogen fixation product dominated by NO_3^- is produced in large-scale aerosol (mist) flows (Figure 5). The unique energy concentration in droplet microreactors leads to the increased energy efficiency at a larger scale compared to the common lab-scale plasma reactors. Compatibility with direct solar power, flow-reactor chemistry, and electrified processes at industry-relevant scales make this low-cost, low-carbon-footprint, renewable-energy-driven process and system promising for the widespread sustainable and distributed production and applications of plasma nitrogen fixation [19].

5.1 | Large-Throughput Charged Water Flows

Several applications require treatment or utilization of large water volumes, often above several hundreds or thousands of kilograms per hour. For example, in agriculture, large amounts of water-based solutions containing chemicals such as pesticides, herbicides, or fertilizer must be spread on cultivated fields. In the process and manufacturing industries, the production of large-scale commodities is based on large production plants, which, among the raw materials, usually include noticeable amounts of industry-grade water. For these applications, the use of small-scale ES needles or mist generators poses noticeable challenges because of the number of units to be placed in parallel, the distance at which they should be kept to avoid mutual interferences, and the corresponding specific surface area per unit flow rate required. Besides, apart from a few cases, the operating conditions of agricultural or industrial processes imply the presence of gas flows and the unavoidable entrainment of the sprayed droplets into the gas phase. Consequently, the very low average droplet size that represents one of the most important characteristics of traditional Es turns out to be a critical problem because of their easy carryover in the gas stream and their subsequent evaporation. Although this is a potential advantage for some applications (such as evaporation or humidification), this is unacceptable any time the process requires preserving the water in the liquid state.

16128869, 0, Downloaded from https://onlinelibrary.wiley.com/doi/10.1002/ppap.202400275 by Mario Janda - Cochrane Slovakia , Wiley Online Library on [30/12/2024]. See the Terms and Conditions (https://onlinelibrary.wiley.com/terms-and-conditions) on Wiley Online Library for rules of use; OA articles are governed by the applicable Creative Commons License

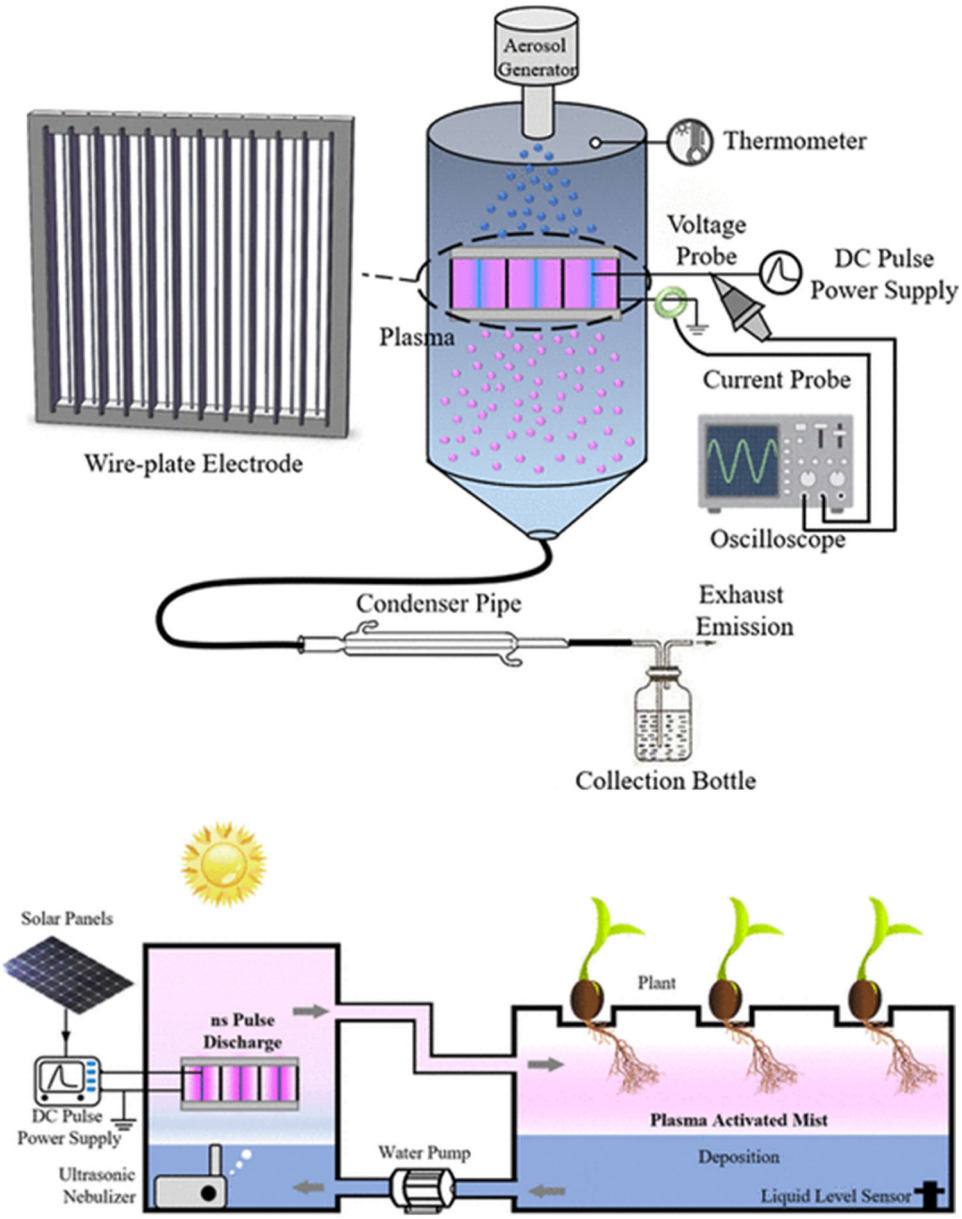

FIGURE 5 | Example schematic of the continuous, plasma-droplets, nitrogen fixation system. Mist droplets were generated by an ultrasonic nebulizer. The plasma was a uniform plasma array; the products were collected by a low-temperature condensation system. The PAM-aeroponics system includes the PAM nitrogen fixation system, an ultrasonic nebulizer, a water tank, and a plant stand. The solar panel is used to drive the PAM system. Reprinted from [19] with permissions from American Chemical Society, 2024.

For these applications, the electrospraying process should be tuned to generate droplets with the highest possible charge-to-mass ratio achievable for a droplet size distribution acceptable for the specific application. For example, in agricultural applications, this often led to the use of pneumatic nozzles generating droplets above 100 μm, whereas in process or manufacturing industries, both pneumatic and hydraulic nozzles are used to generate droplets with a size range from tens to hundreds of micrometers depending on the specific application. The typical flow rates of these units are from tenths to tens L/min and induction charging is often the preferred choice for electrification because of the easier management of high-voltage lines.

By reversing the perspective, the generation of plasma for water sprays deriving from high flow rates is highly desirable because of the possibility of extending the plasma-based processes to several large-scale applications, such as wastewater treatment, water remediation processes, or wet oxidation scrubbing. Although the formation of corona discharges in large flow rate nozzles has been reported in the literature, to the best of our knowledge, there are still no applications on plasma processes for such systems.

Up-scaling of plasma–aerosol systems for flow rate nozzles above L/min is still at an early stage because of the limited charge density that can be transferred to the spray compared with that achievable for ESs operating in cone jet mode. This is particularly evident for induction spray nozzles and derives essentially from the fact that the operation of large water flow rate nozzles implies that the liquid jet thickness and droplet size

16128868, 0, Downloaded from https://onlinelibrary.wiley.com/doi/10.1002/ppap.202400275 by Mario Janda - Cochrane Slovakia , Wiley Online Library on [30/12/2024]. See the Terms and Conditions (https://onlinelibrary.wiley.com/terms-and-conditions) on Wiley Online Library for rules of use; OA articles are governed by the applicable Creative Commons License

are in the size range of hundreds of micrometers. Larger liquid jet and droplets imply lower surface to volume ratio and consequently lower charge density. This is because, during the induction charging, a separation of charge in the liquid occurs thanks to the application of an external electric field at the high-voltage electrode. According to the leaky dielectric liquid model [123], the liquid polarizes under the effect of the electric field: either negative or positive ions accumulate at the liquid jet/sheet interface depending on the sign of the potential fixed at the high-voltage electrode, whereas the same number of ions with the opposite sign accumulates in the bulk of the liquid. Under the effect of applied pressure and auxiliary air (for pneumatic nozzles), the liquid jet/sheet stretches, and its thickness is reduced from the nozzle exit section to the liquid tip. When atomization takes place, the liquid jet/sheet breaks and charge separation occurs, forming droplets that carry a net charge with a sign equal to that of the ions accumulated on the jet/sheet surface. This spray of charged droplets corresponds to a net current flowing from the jet/sheet to the environment. Because of induction, an opposite current travels from the liquid sheet to the grounded surface of the nozzle. Experiments revealed that for both hydraulic and pneumatic nozzles, the induction current is an almost linear function of the applied potential.

Nevertheless, above a certain potential, the onset of gas discharges in the space between the charged electrode and the liquid jet/sheet has been observed. For example, Marchewicz et al. showed that for both hollow cone and full cone induction charging hydraulic sprays, corona discharges appear when the potential applied to the high-voltage electrode crosses a critical level [124]. The same result has been observed by Di Natale et al. [125] and Manna et al. [126] As suggested by Higashiyama et al. [127] and Castle and Inculet [128] and later reported by Marchewicz et al. [124], when the critical potential is overcome, corona discharges occur between the charging electrode and the liquid jet. Manna [129] and Di Bonito et al. [130] have investigated the balancing of electric current in an induction charged spray by including in the analysis not only the spray current but also the ground current flowing through the nozzle and the one provided by the high-voltage generator, when such corona discharges appear.

When time-average values of the spray current are measured, the experiments revealed that on increasing the potential above this critical value, the spray current decreased, eventually reaching zero and even reversing its signs. Experiments carried out by Di Bonito et al. using high-frequency measurements of the spray current indicate the presence of discharges in the form of current peaks, Trichel pulses, having a sign opposite to the induction current (see Figure 6) [130]. On increasing the applied potential, the induction current increases, as also the discharges' frequency and intensity. Consequently, the average current decreases. At higher potentials, the discharges prevail, finally overwhelming the induction current.

One of the most interesting experimentally confirmed features of the process is that the corona discharge current flows both in the liquid film and in the spray droplets. Differently from the induction charging, in this case, the discharge current flows from the gas to the liquid, contributing to both the current flowing in the liquid jet/sheet and the sprayed droplets in similar proportions.

The onset of gas ionization phenomena is achieved when the electric field between the liquid jet and the high-voltage electrode overcomes the breakdown potential of humid air. This condition depends on several aspects: (i) the voltage applied to the charging electrode; (ii) the distance between the electrode and the tip of the liquid jet/sheet; and (iii) the characteristics of the humid gas in between.

As the electrodes usually have a blunt shape, gas discharges are likely triggered by the presence of a high-curvature surface at the jet/sheet tip or due to the presence of a water layer on the surface of the high-voltage electrode. Under these conditions, it is likely that plasma processes can also take place in large-scale sprays; however, to the best of our knowledge, there are no reported applications of this kind in the pertinent literature and more experimental research is needed to support development of the plasma process with large flow rate nozzles.

For further development, comparison with competitive technologies (e.g., spraying PAW produced by bulk liquid treatment; aerosols of chemical solutions) is a necessary aspect of any study focused on scale-up and optimization of plasma–aerosol systems. Parameters such as energy yield, water consumption, treatment capacity, and treatment cost [6], together with any other indicator used in the specific application, are essential to promote advancement of the PAA technology. Unfortunately, to date, there is still not enough information on large-scale units to properly address the quantitative values of these parameters.

6 | Controversies

6.1 | Is It Worth Using Aerosol Interacting with Plasma?

One argument for converting water into an aerosol is to increase the interface between the gaseous and liquid phases. By converting bulk water into microdroplets, one can indeed increase the active surface area by several orders of magnitude. However, the amount of chemicals dissolved in the microdroplets does not depend solely on the size of this surface. Another important parameter is the interaction time [48]. When comparing the transport of particles from gas to water and to microdroplets, it is therefore more appropriate to use the product of the interface area and the interaction time. For example, microdroplets generated during electrospraying pass through the gas phase at a relatively high speed and attach on the reactor walls after a few milliseconds. The value of the product of area and interaction time is smaller than if the same volume of water without spraying was in contact with the gas containing RONS for 1 min [48].

It is also necessary to consider what happens to the microdroplets after they encounter the surfaces in the reactor. In the case of a continuous supply of new microdroplets, their accumulation can create a layer of bulk water directly in the reactor. In this case, the transport of reactive species from the

16128869, 0, Downloaded from https://onlinelibrary.wiley.com/doi/10.1002/ppap.202400275 by Mario Janda - Cochrane Slovakia , Wiley Online Library on [30/12/2024]. See the Terms and Conditions (https://onlinelibrary.wiley.com/terms-and-conditions) on Wiley Online Library for rules of use; OA articles are governed by the applicable Creative Commons License

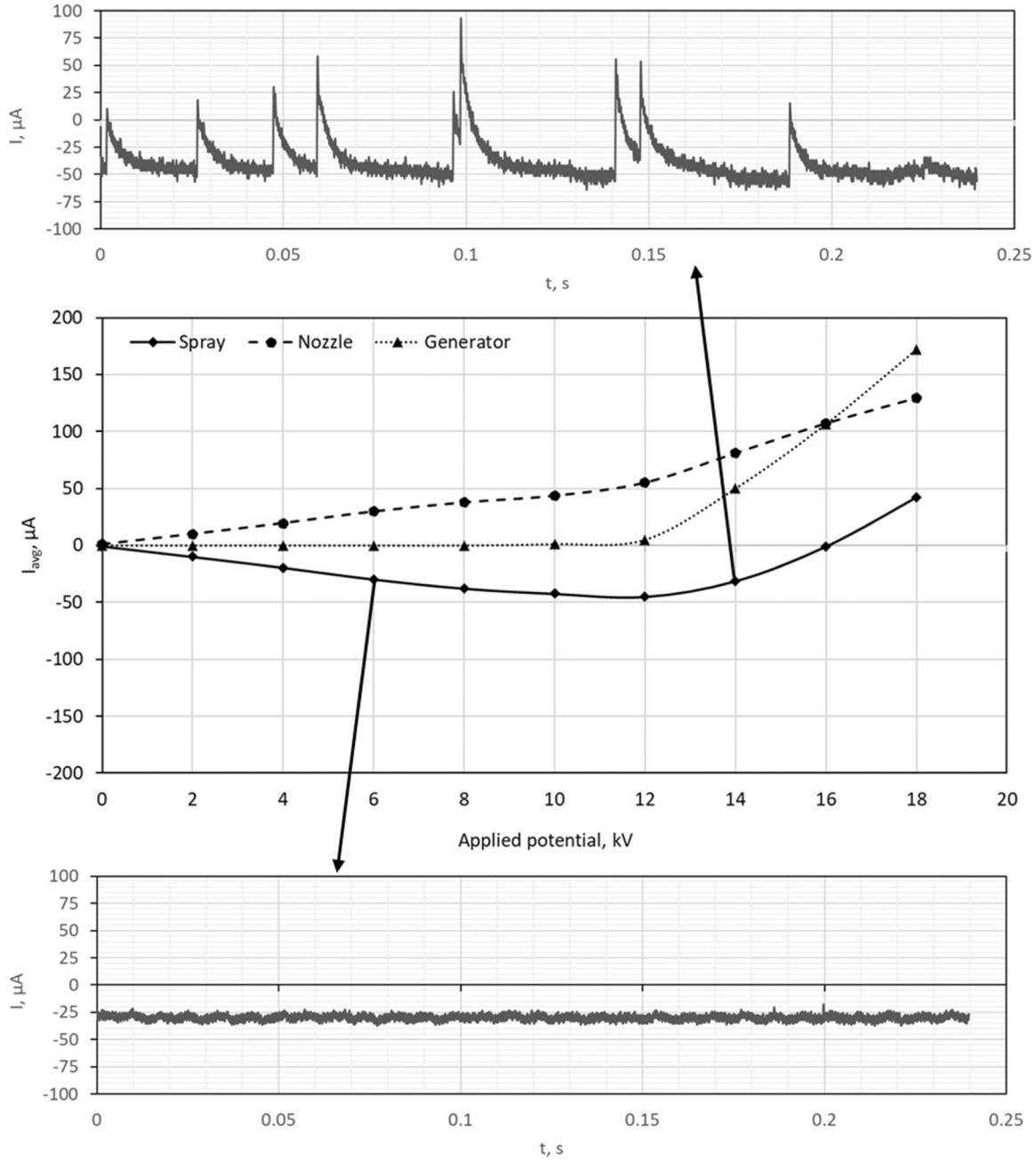

FIGURE 6 | Average spray current (central figure) of an induction charging for a Spraying System Unijet SS 6510 flat spray nozzle with tap water, with current signals for pure induction charging (6 kV bottom figure) and Trichel pulses above the critical potential (14 kV, top figure). Data are from Di Bonito et al. [130].

gas occurs both to the surface microdroplets and to the bulk water. If the experiment with the accumulation of water from microdroplets lasts a minute or more, more chemicals can dissolve in the water while it is in the form of surface microdroplets or bulk water in the reactor than passing through volume microdroplets. For this reason, it remains controversial as to whether it makes sense to convert water into microdroplets in volume or to increase the product of interaction time and area by having the water form thin films on the surface of the electrodes; also, the interaction time of the water with the gas would be significantly longer than a few milliseconds. This thin-film plasma–water treatment has been adopted, for example, in [131].

In the case of an aerosol produced by a nebulizer, the total volume of water in the reactor can be relatively small and the ultrafine microdroplets that condense on the surfaces will not create bulk water in the reactor but will evaporate. In this case, the subsequent sampling is a problem. By passing the gas with aerosol behind the reactor through an ice bath, a condensate is formed, which consists not only of the sampled microdroplets but also the initial gas moisture. In certain cases, the gas moisture may contribute more to the collected condensed sample than the microdroplets [132]. This reduces the significance of the obtained results if the efficiency of the transport of reactive gas particles to microdroplets were to be estimated from such experiments.

16128869, 0, Downloaded from https://onlinelibrary.wiley.com/doi/10.1002/ppap.202400275 by Mario Janda - Cochrane Slovakia , Wiley Online Library on [30/12/2024]. See the Terms and Conditions (https://onlinelibrary.wiley.com/terms-and-conditions) on Wiley Online Library for rules of use; OA articles are governed by the applicable Creative Commons License

In addition to the size of the interface surface and the duration of the plasma–aerosol interaction time, the charge of the microdroplets can also influence the dissolution of various chemicals. This is indicated by experiments comparing the solubility of several RONS in uncharged microdroplets from a nebulizer and charged microdroplets from ES [49]. However, this influence has not yet been sufficiently investigated and requires further experiments.

Furthermore, it is crucial to recognize that the total plasma–liquid interface area increases not only by decreasing the diameter of microdroplets but also by increasing their density in the gas. This increased aerosol density can enhance the overall mass transfer of all species from the gas to the liquid. Wang et al. demonstrated this effect, showing that increased spray density significantly improved the removal of small dust particles (<10 μm) from air [133]. However, increasing aerosol density can negatively impact electrical discharge stability, potentially reducing the production of gaseous RONS. Therefore, further research should investigate the complex interplay between electrical discharges and high-density water aerosols.

Finally, the relevance of using water sprayed into microdroplets is questionable if the goal is to dissolve highly soluble chemicals such as H_2O_2 and HNO_3. For these compounds, the limiting factor may not be the size of the interface, but their concentration in the gas phase. Due to dissolution into microdroplets, a significant local decrease in their gas-phase concentration can occur, and this can limit the total amount that dissolves in the water.

6.2 | Charge Effects on Microdroplets, Species Chemistry, and Transport

In natural atmospheric clouds, water droplets grow by condensation in a supersaturated water vapor environment. Under subsaturated conditions, water droplets normally continue to evaporate until they eventually disappear. In contrast, Zhang et al. have shown that the formation of mist droplets visible to the naked eye could be induced by direct current corona discharge under supersaturated conditions. They found that corona discharge could promote the growth of water droplets even under subsaturated conditions. Possible mechanisms are discussed, but not fully understood, and their results suggest that the droplet growth enhancement is supported by the synergetic effects of droplet surface charge, external electric field, and ionic wind generated by the corona discharge [134].

The plasma activation of droplets depends on the transport of the droplets through the plasma, which in turn depends on their ambipolar charging. Nayak et al. report on the transport dynamics of water droplets, tens of microns in diameter, carried by the gas flow through an atmospheric pressure radiofrequency glow discharge sustained in helium. The droplets pass through the plasma with minimal evaporation and without reaching the Rayleigh limit. The measurements of the droplet trajectory were analyzed using results from a three-dimensional fluid model and a two-dimensional plasma hydrodynamics model. It was found that the transport dynamics as the droplet enters and leaves the plasma are due to differential charging of the droplet in the plasma gradients of the bounding sheaths to the plasma [135].

Besides charge physical effects on the droplet motion and coagulation, the results of Hassan et al. indicate that ES (charged aerosol) enhances the transport of RNS (NO_2 and HNO_2 that form NO_2^- on entering water) and not ROS (H_2O_2, O_3) with respect to non-charged nebulized aerosol. NO_2^- ion formation efficiency was strongly improved in ES microdroplets with respect to bulk water and even nebulized microdroplets, which is likely due to the charge effect that enhanced the formation of aqueous nitrite NO_2^- ions when NO_2 or HNO_2 are transported into water. This may indicate that charged ESs solvating RONS that are not ionic in the gas (e.g., HNO_2, NO_2) but are converted into ions upon entering water (NO_2^-) enhance this transport. More investigations must be conducted, for example, focusing on the effect of ES microdroplet polarity. So far, these experiments have only been carried out with positively charged ES microdroplets with respect to negative ion formation (NO_2^-) [49].

6.3 | Is the Ex Situ Water Diagnostic Useful for Understanding the Transport of RONS?

The transport of RONS from plasma to water and their formation in PAW/PAA and all its scientific and diagnostics challenges have been discussed previously in Sections 2 and 3. Despite the fact that it is crucial to analyze the composition of PAAs by accumulating them as a measurable amount of bulk liquid, the drawback of such indirect ex situ diagnostics is the relatively long time needed to accumulate enough condensed aerosol microdroplets for further analysis. During this time, partial conversion of solvated RONS can occur, which is influenced by liquid-phase reactions, for example, by a disproportionation reaction converting NO_2^- into NO_3^- at lower pH [80]. Accumulation of aerosol microdroplets to obtain enough volume for liquid analysis, for example, in an ice bath, as done by Hassan et al. [49], takes too long a time. During this time, the condensing treated aerosol is necessarily also influenced by the condensing background water vapor, which may intrinsically dilute the measured concentrations of RONS. On the other hand, ex situ yet online diagnostics can effectively represent the transfer of RONS and charges from PAA droplets to application targets, such as plants, seeds, or food products. Such diagnostics are crucial for applications, as they enable the optimization of parameters like droplet size and velocity to ensure their effective distribution on target surfaces, which often possess unique morphologies and properties.

7 | Proposed Path and Outlook

Despite the above-mentioned challenges, significant progress has been made in understanding the transport of reactive species from CAP to water. This has led to the development of more efficient plasma-based water treatment technologies and applications in biomedicine and agriculture.

The advantage of plasma process applications is intrinsically related to the possibility of in situ generation of the chemicals required for the process, such that the production costs associated with their production are decreased and the

16128868, 0, Downloaded from https://onlinelibrary.wiley.com/doi/10.1002/ppap.202400275 by Mario Janda - Cochrane Slovakia , Wiley Online Library on [30/12/2024]. See the Terms and Conditions (https://onlinelibrary.wiley.com/terms-and-conditions) on Wiley Online Library for rules of use; OA articles are governed by the applicable Creative Commons License

corresponding impacts on the environment are eliminated. This has potential benefits for the life cycle assessment of the plasma process, although the management of by-products still requires further research for a complete understanding of their impacts. Compared to other configurations for plasma-treated water, the use of aerosol yields the advantage of the possibility to produce PAW on demand and directly on the target without the need for storage.

The transport of RONS from plasma to water bulk/films/aerosols has been studied both numerically and experimentally. The key transport phenomena have been identified and it was acknowledged that some species are transported easily even into bulk water (H_2O_2, HNO_3), but some are significantly enhanced by aerosolization (O_3, NO, NO_2, OH). Many phenomena and controversies must still be addressed to fully understand and tune the process of plasma–microdroplet interactions, which will lead to "niche" applications and up-scaling.

A deeper understanding of plasma–aerosol interaction phenomena may also be very helpful for analytical chemistry applications, for example, when samples with trace contaminants in the form of liquid aerosols are introduced into a microwave or inductively coupled plasma for atomic spectroscopy [136].

New/modified diagnostic techniques are crucial for advancing our understanding of plasma interactions with water aerosols. In situ methods are particularly important for real-time analysis during the interaction process. These techniques should provide valuable insights into the chemical composition of microdroplets and/or their surface chemistry. In situ diagnostics can reveal the dynamics of chemical reactions at the droplet surface.

Investigation of the interaction of plasma with water aerosols requires precise control over microdroplet generation. To advance basic research in this area, improvements in droplet generation tools are essential. Ideally, these tools should produce on-demand microdroplets with specific, selectable diameters. This level of control would allow researchers to isolate the effects of droplet size on plasma interaction. Alternatively, enhancing existing diagnostic tools can provide valuable insights. For instance, synchronization of Raman light sheet micro-spectroscopy with microdroplet formation can reveal real-time chemical changes.

Understanding the plasma–water aerosol interactions could also be improved by developing techniques for more precise control over microdroplet positioning within the reaction zone. Acoustic levitators, for example, offer a promising solution for capturing and stabilizing microdroplets in the plasma environment.

Furthermore, insights into plasma–aerosol interactions can enhance our understanding of the mutual influence between plasma and aerosols. This knowledge can drive the development of novel reactor designs that maximize the interaction surface area and enhance mass transfer while minimizing any negative impact on plasma reactivity. Such optimization can lead to faster processing times and increased production rates of PAA.

Plasma–aerosol systems hold the potential to overcome some of the up-scaling issues encountered while using other plasma configurations to produce PAW. Although the feasibility for mass production of PAW with high concentrations of long reactive species from plasma–aerosols remains uncertain, the adoption of this solution offers an alternative approach with other advantages: on-demand production of aerosol charged with short-lived reactive species directly delivered to the target; treatment of large areas in a continuous way; and low water consumption. *Scale-up* attempts should focus on optimizing these advantages of the technology when compared to other solutions. In particular, comparison with competitive technologies (e.g., spraying PAW produced by bulk treatment; aerosols of chemical solutions) is a necessary aspect of any study focused on scale-up and optimization. Indicators such as energy yield, water consumption, treatment capacity, and treatment cost [6], together with any other indicator used in the specific application, are essential for further advancement of the technology. Thus, *exploration of novel applications* where PAAs are utilized directly, before condensation into bulk water, is crucial and can be considered as another proposed path outlook. One promising avenue lies in air purification, where airborne pollutants could be neutralized by reactive species within the activated aerosol. This approach could be used in ventilation systems or localized air treatment devices, for example, to remove oil mist emitted from cooking devices, which represents a major source of atmospheric particulate matter in urban areas [18]. In the food industry, PAAs (fog) could be used for the preservation and decontamination of produce that cannot be treated by bulk water, extending the shelf-life and reducing spoilage [137].

Once a suitable application is identified, a more in-depth understanding of plasma–water–aerosol interactions can enable optimized PAW/PAA formation. By studying how plasma species interact with water droplets, we can enhance the efficiency and tailor the composition of PAW. For instance, optimizing plasma and aerosol parameters can lead to higher concentrations of desired compounds in PAW/PAA. This knowledge allows for the *fine-tuning of PAW/PAA composition*, enabling the production of specific RONS for targeted applications.

On the other hand, the applicability of plasma–aerosol technology has a current limitation in the flow rate that can be provided by a single nozzle. This limits the scale of the process that can be expanded with this technique. New nozzle designs allowing for high-throughput aerosolized liquid flows need to be developed further.

In conclusion, cold plasma and aerosol are two technologies that have great potential to improve one another. Instead of small plasmas treating large volumes of water to be stored and used later, plasma–aerosol systems produce an activated aerosol to treat large areas directly. Instead of chemicals that are produced, transported, stored, and later atomized, plasma–aerosol systems produce chemicals on the spot, moments before their applications. Far from being trivial, optimizing the matching of cold plasma and aerosol technologies has the potential to create new solutions for many future applications.

Acknowledgments

This study was funded by the EU NextGenerationEU through the Recovery and Resilience Plan for Slovakia under the project No. 09I03-

16128868, 0, Downloaded from https://onlinelibrary.wiley.com/doi/10.1002/ppap.202400275 by Mario Janda - Cochrane Slovakia , Wiley Online Library on [30/12/2024]. See the Terms and Conditions (https://onlinelibrary.wiley.com/terms-and-conditions) on Wiley Online Library for rules of use; OA articles are governed by the applicable Creative Commons License

03-V03-00033 EnvAdwice and ANR-23-CE04-0003 "PLASMASOL—Cold plasma and water aerosol: A new eco-friendly tool for agriculture", and is based upon collaboration within COST Action CA20114 PlasTHER, supported by COST (European Cooperation in Science and Technology).

Data Availability Statement

The data that support the findings of this study are available on request from the corresponding author. The data are not publicly available due to privacy or ethical restrictions.

References

1. M. L. Pöhlker, C. Pöhlker, O. O. Krüger, et al., "Respiratory Aerosols and Droplets in the Transmission of Infectious Diseases," *Reviews of Modern Physics* 95 (2023): 045001, https://doi.org/10.1103/RevModPhys.95.045001.

2. J. Atkinson, Y. Chartier, C. L. Pessoa-Silva, P. Jensen, Y. Li, and W.-H. Seto, *Natural Ventilation for Infection Control in Health-Care Settings* (Geneva: World Health Organization, 2009).

3. P. Rogliani, L. Calzetta, A. Coppola, et al., "Optimizing Drug Delivery in COPD: The Role of Inhaler Devices," *Respiratory Medicine* 124 (2017): 6–14, https://doi.org/10.1016/j.rmed.2017.01.006.

4. F. Anlimah, V. Gopaldasani, C. MacPhail, and B. Davies, "A Systematic Review of the Effectiveness of Dust Control Measures Adopted to Reduce Workplace Exposure," *Environmental Science and Pollution Research* 30 (2023): 54407–54428, https://doi.org/10.1007/s11356-023-26321-w.

5. F. Ahmad, A. Khaliq, B. Qiu, M. Sultan, and J. Ma, "Advancements of Spraying Technology in Agriculture," in *Technology in Agriculture*, eds. F. Ahmad and M. Sultan (IntechOpen, 2021), https://doi.org/10.5772/intechopen.98500.

6. F. Bilea, M. Garcia-Vaquero, M. Magureanu, et al., "Non-Thermal Plasma as Environmentally-Friendly Technology for Agriculture: A Review and Roadmap," *Critical Reviews in Plant Sciences* 43 (2024): 428–486, https://doi.org/10.1080/07352689.2024.2410145.

7. C. Bradu, K. Kutasi, M. Magureanu, N. Puač, and S. Živković, "Reactive Nitrogen Species in Plasma-Activated Water: Generation, Chemistry and Application in Agriculture," *Journal of Physics D: Applied Physics* 53 (2020): 223001, https://doi.org/10.1088/1361-6463/ab795a.

8. N. K. Kaushik, B. Ghimire, Y. Li, et al., "Biological and Medical Applications of Plasma-Activated Media, Water and Solutions," *Biological Chemistry* 400 (2018): 39–62, https://doi.org/10.1515/hsz-2018-0226.

9. B. R. Locke and K.-Y. Shih, "Review of the Methods to Form Hydrogen Peroxide in Electrical Discharge Plasma With Liquid Water," *Plasma Sources Science and Technology* 20 (2011): 034006, https://doi.org/10.1088/0963-0252/20/3/034006.

10. Y. Li, L. Wei, J. Lin, et al., "Nonthermal Plasma Air Disinfection for the Inactivation of Airborne Microorganisms in an Experimental Chamber and Indoor Air," *Journal of Applied Microbiology* 135 (2024): lxae078, https://doi.org/10.1093/jambio/lxae078.

11. U. Schmelz, T. Schaal, G. Hämmerle, and T. Tischendorf, "The Further Development of Cold Plasma Technology: The Effectiveness of a Contactless, Indirect Atmospheric Cold Plasma Method for Germ Reduction on Surfaces In Vitro and In Vivo," 2024, https://doi.org/10.1101/2024.10.12.24315382.

12. Z. Ma, A. K. Dwivedi, and H. L. Clack, "Effects of Chemically-Reductive Trace Gas Contaminants on Non-Thermal Plasma Inactivation of an Airborne Virus," *Science of the Total Environment* 939 (2024): 173447, https://doi.org/10.1016/j.scitotenv.2024.173447.

13. Z. Machala, B. Tarabova, K. Hensel, E. Spetlikova, L. Sikurova, and P. Lukes, "Formation of ROS and RNS in Water Electro-Sprayed through Transient Spark Discharge in Air and Their Bactericidal Effects: Formation of ROS/RNS in Water Sprayed through Spark in Air," *Plasma Processes and Polymers* 10 (2013): 649–659, https://doi.org/10.1002/ppap.201200113.

14. P. Ranieri, G. McGovern, H. Tse, et al., "Microsecond-Pulsed Dielectric Barrier Discharge Plasma-Treated Mist for Inactivation of *Escherichia Coli* In Vitro," *IEEE Transactions on Plasma Science* 47 (2019): 395–402, https://doi.org/10.1109/TPS.2018.2878971.

15. A. Bisag, P. Isabelli, R. Laurita, et al., "Cold Atmospheric Plasma Inactivation of Aerosolized Microdroplets Containing Bacteria and Purified SARS-CoV-2 RNA to Contrast Airborne Indoor Transmission," *Plasma Processes & Polymers* 17 (2020): 2000154, https://doi.org/10.1002/ppap.202000154.

16. B. Chen, Y. Wang, S. Li, N. Xu, and Y. Fu, "Environment Pollutants Removal With Non-Thermal Plasma Technology," *International Journal of Low-Carbon Technologies* 17 (2022): 446–455, https://doi.org/10.1093/ijlct/ctac016.

17. A. Dorosz, A. Penconek, and A. Moskal, "Cold Plasma Gliding Arc Reactor System for Nanoparticles' Removal From Diesel Cars' Exhaust Gases," *Processes* 12 (2024): 1841, https://doi.org/10.3390/pr12091841.

18. M. S. Kang, G. Yu, J. Shin, and J. Hwang, "Collection and Decomposition of Oil Mist Via Corona Discharge and Surface Dielectric Barrier Discharge," *Journal of Hazardous Materials* 411 (2021): 125038, https://doi.org/10.1016/j.jhazmat.2021.125038.

19. H. Gao, G. Wang, Z. Huang, et al., "Plasma-Activated Mist: Continuous-Flow, Scalable Nitrogen Fixation, and Aeroponics," *ACS Sustainable Chemistry & Engineering* 11 (2023): 4420–4429, https://doi.org/10.1021/acssuschemeng.2c07324.

20. Y. Zhang, H. Cheng, H. Gao, D. Liu, and X. Lu, "On the Charged Aerosols Generated By Atmospheric Pressure Non-Equilibrium Plasma," *High Voltage* 6 (2021): 408–425, https://doi.org/10.1049/hve2.12036.

21. F. Massines, C. Sarra-Bournet, F. Fanelli, N. Naudé, and N. Gherardi, "Atmospheric Pressure Low Temperature Direct Plasma Technology: Status and Challenges for Thin Film Deposition," *Plasma Processes & Polymers* 9 (2012): 1041–1073, https://doi.org/10.1002/ppap.201200029.

22. Y.-S. Lin, W.-C. Zhong, G.-M. Zhang, and P.-T. Chen, "Cold Atmospheric Pressure Plasma-Assisted Aerosol Deposition of Multi-Colored Dual Band Electrochromic $VO_xC_yN_z$ Thin Films," *Solar Energy Materials and Solar Cells* 275 (2024): 113030, https://doi.org/10.1016/j.solmat.2024.113030.

23. T. M. Khan, G. A. S. Alves, and A. Iqbal, "Processing Laser Ablated Plasmonic Nanoparticle Aerosols With Nonthermal Dielectric Barrier Discharge Jets of Argon and Helium and Plasma Induced Effects," *Scientific Reports* 13 (2023): 77, https://doi.org/10.1038/s41598-022-27294-5.

24. P. Maguire, D. Rutherford, M. Macias-Montero, et al., "Continuous In-Flight Synthesis for On-Demand Delivery of Ligand-Free Colloidal Gold Nanoparticles," *Nano Letters* 17 (2017): 1336–1343, https://doi.org/10.1021/acs.nanolett.6b03440.

25. G. Taylor, "Disintegration of Water Drops in an Electric Field," *Proceedings of the Royal Society of London, Series A: Mathematical and Physical Sciences* 280 (1964): 383–397, https://doi.org/10.1098/rspa.1964.0151.

26. M. Cloupeau and B. Prunet-Foch, "Electrostatic Spraying of Liquids: Main Functioning Modes," *Journal of Electrostatics* 25 (1990): 165–184, https://doi.org/10.1016/0304-3886(90)90025-Q.

27. R. P. A. Hartman, D. J. Brunner, D. M. A. Camelot, J. C. M. Marijnissen, and B. Scarlett, "Jet Break-Up in Electrohydrodynamic Atomization in the Cone-Jet Mode," *Journal of Aerosol Science* 31 (2000): 65–95, https://doi.org/10.1016/S0021-8502(99)00034-8.

28. L. Rayleigh. On the Equilibrium of Liquid Conducting Masses Charged With Electricity, The Philosophical Magazine (London: Taylor & Francis, 1882), 184–186.

16128868, 0, Downloaded from https://onlinelibrary.wiley.com/doi/10.1002/ppap.202400275 by Mario Janda - Cochrane Slovakia , Wiley Online Library on [30/12/2024]. See the Terms and Conditions (https://onlinelibrary.wiley.com/terms-and-conditions) on Wiley Online Library for rules of use; OA articles are governed by the applicable Creative Commons License

29. K.-Y. Li, H. Tu, and A. K. Ray, "Charge Limits on Droplets during Evaporation," *Langmuir* 21 (2005): 3786–3794, https://doi.org/10.1021/la047973n.

30. A. Stancampiano, T. Gallingani, M. Gherardi, et al., "Plasma and Aerosols: Challenges, Opportunities and Perspectives," *Applied Sciences* 9 (2019): 3861, https://doi.org/10.3390/app9183861.

31. P. J. Bruggeman, M. J. Kushner, B. R. Locke, et al., "Plasma–Liquid Interactions: A Review and Roadmap," *Plasma Sources Science and Technology* 25 (2016): 053002, https://doi.org/10.1088/0963-0252/25/5/053002.

32. X. Lu, G. V. Naidis, M. Laroussi, S. Reuter, D. B. Graves, and K. Ostrikov, "Reactive Species in Non-Equilibrium Atmospheric-Pressure Plasmas: Generation, Transport, and Biological Effects," *Physics Reports* 630 (2016): 1–84, https://doi.org/10.1016/j.physrep.2016.03.003.

33. A. Schmidt-Bleker, R. Bansemer, S. Reuter, and K.-D. Weltmann, "How to Produce an NOx-Instead of O x-Based Chemistry With a Cold Atmospheric Plasma Jet," *Plasma Processes and Polymers* 13 (2016): 1120–1127, https://doi.org/10.1002/ppap.201600062.

34. M. J. Pavlovich, D. S. Clark, and D. B. Graves, "Quantification of Air Plasma Chemistry for Surface Disinfection," *Plasma Sources Science and Technology* 23 (2014): 065036, https://doi.org/10.1088/0963-0252/23/6/065036.

35. W. Wang, B. Patil, S. Heijkers, V. Hessel, and A. Bogaerts, "Nitrogen Fixation By Gliding Arc Plasma: Better Insight By Chemical Kinetics Modelling," *Chemsuschem* 10 (2017): 2145–2157, https://doi.org/10.1002/cssc.201700095.

36. M. Janda, K. Hensel, Z. Machala, and T. A. Field, "The Influence of Electric Circuit Parameters on NOx Generation By Transient Spark Discharge," *Journal of Physics D: Applied Physics* 56 (2023): 485202, https://doi.org/10.1088/1361-6463/ace634.

37. D. X. Liu, P. Bruggeman, F. Iza, M. Z. Rong, and M. G. Kong, "Global Model of Low-Temperature Atmospheric-Pressure He + H_2O Plasmas," *Plasma Sources Science and Technology* 19 (2010): 025018, https://doi.org/10.1088/0963-0252/19/2/025018.

38. K. Takahashi, Y. Takeuchi, and Y. Matsumi, "Rate Constants of the O(1D) Reactions With N_2, O_2, N_2O, and H_2O at 295 K," *Chemical Physics Letters* 410 (2005): 196–200, https://doi.org/10.1016/j.cplett.2005.05.062.

39. A. S. Viner, P. A. Lawless, D. S. Ensor, and L. E. Sparks, "Ozone Generation in DC-Energized Electrostatic Precipitators," *IEEE Transactions on Industry Applications* 28 (1992): 504–512, https://doi.org/10.1109/28.137427.

40. K. C. Hsieh, R. J. Wandell, S. Bresch, and B. R. Locke, "Analysis of Hydroxyl Radical Formation in a Gas-Liquid Electrical Discharge Plasma Reactor Utilizing Liquid and Gaseous Radical Scavengers," *Plasma Processes & Polymers* 14 (2017): 1600171, https://doi.org/10.1002/ppap.201600171.

41. R. Atkinson, D. L. Baulch, R. A. Cox, R. F. Hampson, J. A. Kerr (Chairman), and J. Troe, "Evaluated Kinetic and Photochemical Data for Atmospheric Chemistry: Supplement III. IUPAC Subcommittee on Gas Kinetic Data Evaluation for Atmospheric Chemistry," *Journal of Physical and Chemical Reference Data* 18 (1989): 881–1097, https://doi.org/10.1063/1.555832.

42. M. Janda, Z. Machala, A. Niklová, and V. Martišovitš, "The Streamer-To-Spark Transition in a Transient Spark: A DC-Driven Nanosecond-Pulsed Discharge in Atmospheric Air," *Plasma Sources Science and Technology* 21 (2012): 045006, https://doi.org/10.1088/0963-0252/21/4/045006.

43. P. Pareek, S. Kooshki, P. Tóth, and M. Janda, "Tuning Composition of Plasma Activated Water Generated By Transient Spark Discharge With Electrospray," *Chemical Engineering Journal* 493 (2024): 152583, https://doi.org/10.1016/j.cej.2024.152583.

44. A. Komuro, R. Ono, and T. Oda, "Behaviour of OH Radicals in an Atmospheric-Pressure Streamer Discharge Studied By Two-Dimensional Numerical Simulation," *Journal of Physics D: Applied Physics* 46 (2013): 175206, https://doi.org/10.1088/0022-3727/46/17/175206.

45. Y. Yang, Z. Li, L. Nie, and X. Lu, "Effect of Liquid-Dissolved Gas Components on Concentrations of the Aqueous Reactive Oxygen and Nitrogen Species," *Journal of Applied Physics* 125 (2019): 223302, https://doi.org/10.1063/1.5085258.

46. R. Sander, "Compilation of Henry's Law Constants (Version 5.0.0) for Water as Solvent," *Atmospheric Chemistry and Physics* 23 (2023): 10901–12440, https://doi.org/10.5194/acp-23-10901-2023.

47. F. L. Smith and A. H. Harvey, "Avoid Common Pitfalls When using Henry's Law," *Chemical Engineering Progress* 103 (2007): 33.

48. M. Hassan, M. Janda, and Z. Machala, "Transport of Gaseous Hydrogen Peroxide and Ozone into Bulk Water vs. Electrosprayed Aerosol," *Water* 13 (2021): 182, https://doi.org/10.3390/w13020182.

49. M. E. Hassan, M. Janda, and Z. Machala, "Comparison of the Transport of Reactive Nitrogen Plasma Species Into Water Bulk vs. Aerosolized Microdroplets," *Plasma Chemistry and Plasma Processing* (2024), https://doi.org/10.1007/s11090-024-10511-6.

50. M. J. Pavlovich, T. Ono, C. Galleher, et al., "Air Spark-Like Plasma Source for Antimicrobial NOx Generation," *Journal of Physics D: Applied Physics* 47 (2014): 505202, https://doi.org/10.1088/0022-3727/47/50/505202.

51. M. Yusupov, E. C. Neyts, P. Simon, et al., "Reactive Molecular Dynamics Simulations of Oxygen Species in a Liquid Water Layer of Interest for Plasma Medicine," *Journal of Physics D: Applied Physics* 47 (2014): 025205, https://doi.org/10.1088/0022-3727/47/2/025205.

52. M. Sovago, R. Kramer Campen, H. J. Bakker, and M. Bonn, "Hydrogen Bonding Strength of Interfacial Water Determined With Surface Sum-Frequency Generation," *Chemical Physics Letters* 470 (2009): 7–12, https://doi.org/10.1016/j.cplett.2009.01.009.

53. S. Tonini and G. E. Cossali, "An Analytical Model of Liquid Drop Evaporation in Gaseous Environment," *International Journal of Thermal Sciences* 57 (2012): 45–53, https://doi.org/10.1016/j.ijthermalsci.2012.01.017.

54. B. C. Garrett, G. K. Schenter, and A. Morita, "Molecular Simulations of the Transport of Molecules Across the Liquid/Vapor Interface of Water," *Chemical Reviews* 106 (2006): 1355–1374, https://doi.org/10.1021/cr040370w.

55. G. R. Stratton, C. L. Bellona, F. Dai, T. M. Holsen, and S. M. Thagard, "Plasma-Based Water Treatment: Conception and Application of a New General Principle for Reactor Design," *Chemical Engineering Journal* 273 (2015): 543–550, https://doi.org/10.1016/j.cej.2015.03.059.

56. J. Kruszelnicki, A. M. Lietz, and M. J. Kushner, "Atmospheric Pressure Plasma Activation of Water Droplets," *Journal of Physics D: Applied Physics* 52 (2019): 355207, https://doi.org/10.1088/1361-6463/ab25dc.

57. I. Sremački, G. Bruno, H. Jablonowski, C. Leys, A. Nikiforov, and K. Wende, "Influence of Aerosol Injection on the Liquid Chemistry Induced By an RF Argon Plasma Jet," *Plasma Sources Science and Technology* 30 (2021): 095018, https://doi.org/10.1088/1361-6595/abe176.

58. Z. Kovalova, M. Leroy, M. J. Kirkpatrick, E. Odic, and Z. Machala, "Corona Discharges With Water Electrospray for *Escherichia coli* Biofilm Eradication on a Surface," *Bioelectrochemistry* 112 (2016): 91–99, https://doi.org/10.1016/j.bioelechem.2016.05.002.

59. G. Oinuma, G. Nayak, Y. Du, and P. J. Bruggeman, "Controlled Plasma–Droplet Interactions: A Quantitative Study of OH Transfer in Plasma–Liquid Interaction," *Plasma Sources Science and Technology* 29 (2020): 095002, https://doi.org/10.1088/1361-6595/aba988.

16128869, 0, Downloaded from https://onlinelibrary.wiley.com/doi/10.1002/ppap.202400275 by Mario Janda - Cochrane Slovakia , Wiley Online Library on [30/12/2024]. See the Terms and Conditions (https://onlinelibrary.wiley.com/terms-and-conditions) on Wiley Online Library for rules of use; OA articles are governed by the applicable Creative Commons License

60. R. Burlica, R. G. Grim, K. -Y. Shih, D. Balkwill, and B. R. Locke, "Bacteria Inactivation Using Low Power Pulsed Gliding Arc Discharges With Water Spray," *Plasma Processes & Polymers* 7 (2010): 640–649, https://doi.org/10.1002/ppap.200900183.

61. G. Pyrgiotakis, J. McDevitt, A. Bordini, et al., "A Chemical Free, Nanotechnology-Based Method for Airborne Bacterial Inactivation Using Engineered Water Nanostructures," *Environmental Science: Nano* 2014 (2014): 15–26, https://doi.org/10.1039/C3EN00007A.

62. O. Ogunyinka, A. Wright, G. Bolognesi, F. Iza, and H. C. H. Bandulasena, "An Integrated Microfluidic Chip for Generation and Transfer of Reactive Species Using Gas Plasma," *Microfluidics and Nanofluidics* 24 (2020): 13, https://doi.org/10.1007/s10404-019-2316-9.

63. Z. Liu, S. Wang, B. Pang, et al., "The Impact of Surface-To-Volume Ratio on the Plasma Activated Water Characteristics and Its Anticancer Effect," *Journal of Physics D: Applied Physics* 54 (2021): 215203, https://doi.org/10.1088/1361-6463/abe78f.

64. C. C. W. Verlackt, W. Van Boxem, and A. Bogaerts, "Transport and Accumulation of Plasma Generated Species in Aqueous Solution," *Physical Chemistry Chemical Physics* 20 (2018): 6845–6859, https://doi.org/10.1039/C7CP07593F.

65. J. A. Silsby, S. Simon, J. L. Walsh, and M. I. Hasan, "The Influence of Gas–Liquid Interfacial Transport Theory on Numerical Modelling of Plasma Activation of Water," *Plasma Chemistry and Plasma Processing* 41 (2021): 1363–1380, https://doi.org/10.1007/s11090-021-10182-7.

66. S. Keniley, N. B. Uner, E. Perez, R. M. Sankaran, and D. Curreli, "Multiphase Modeling of the DC Plasma–Water Interface: Application to Hydrogen Peroxide Generation With Experimental Validation," *Plasma Sources Science and Technology* 31 (2022): 075001, https://doi.org/10.1088/1361-6595/ac7891.

67. J. Luo, L. Nie, D. Liu, and X. Lu, "Electrodeless Discharge in Water: Reactive Species in Liquid and Gas Phase and Energy Cost for Nitrogen Fixation," *Plasma Processes & Polymers* 20 (2023): 2200181, https://doi.org/10.1002/ppap.202200181.

68. Y. Gorbanev, D. O'Connell, and V. Chechik, "Non-Thermal Plasma in Contact With Water: The Origin of Species," *Chemistry—A European Journal* 22 (2016): 3496–3505, https://doi.org/10.1002/chem.201503771.

69. J. Winter, H. Tresp, M. U. Hammer, et al., "Tracking Plasma Generated H_2 O_2 From Gas into Liquid Phase and Revealing Its Dominant Impact on Human Skin Cells," *Journal of Physics D: Applied Physics* 47 (2014): 285401, https://doi.org/10.1088/0022-3727/47/28/285401.

70. Z. Machala, B. Tarabová, D. Sersenová, M. Janda, and K. Hensel, "Chemical and Antibacterial Effects of Plasma Activated Water: Correlation With Gaseous and Aqueous Reactive Oxygen and Nitrogen Species, Plasma Sources and Air Flow Conditions," *Journal of Physics D: Applied Physics* 52 (2019): 034002, https://doi.org/10.1088/1361-6463/aae807.

71. M. Janda, V. Martišovitš, and Z. Machala, "Transient Spark: a DC-Driven Repetitively Pulsed Discharge and Its Control By Electric Circuit Parameters," *Plasma Sources Science and Technology* 20 (2011): 035015, https://doi.org/10.1088/0963-0252/20/3/035015.

72. S. Kanazawa, H. Kawano, S. Watanabe, et al., "Observation of OH Radicals Produced By Pulsed Discharges on the Surface of a Liquid," *Plasma Sources Science and Technology* 20 (2011): 034010, https://doi.org/10.1088/0963-0252/20/3/034010.

73. P. Bruggeman and D. C. Schram, "On OH Production in Water Containing Atmospheric Pressure Plasmas," *Plasma Sources Science and Technology* 19 (2010): 045025, https://doi.org/10.1088/0963-0252/19/4/045025.

74. X. Zhou, Z. Zhao, J. Liang, H. Yuan, W. Wang, and D. Yang, "Measurement of Reactive Species in Different Solutions of Bubble Discharge With Varying O_2/N_2 Proportion in Ar: Analysis of Reaction Pathways," *Plasma Processes & Polymers* 16 (2019): e1900001, https://doi.org/10.1002/ppap.201900001.

75. H. Taube, "Photochemical Reactions of Ozone in Solution," *Transactions of the Faraday Society* 53 (1957): 656, https://doi.org/10.1039/tf9575300656.

76. S. Xu, V. Jirasek, and P. Lukes, "Molecular Dynamics Simulations of Singlet Oxygen Atoms Reactions With Water Leading to Hydrogen Peroxide," *Journal of Physics D: Applied Physics* 53 (2020): 275204, https://doi.org/10.1088/1361-6463/ab8321.

77. Z. Wang, X. Wang, S. Xu, et al., "Off-Site Production of Plasma-Activated Water for Efficient Disinfection: The Crucial Role of High Valence NOx and New Chemical Pathways," *Water Research* 267 (2024): 122541, https://doi.org/10.1016/j.watres.2024.122541.

78. M. Janda, K. Hensel, P. Tóth, M. E. Hassan, and Z. Machala, "The Role of HNO_2 in the Generation of Plasma-Activated Water By Air Transient Spark Discharge," *Applied Sciences* 11 (2021): 7053, https://doi.org/10.3390/app11157053.

79. J.-L. Brisset and J. Pawlat, "Chemical Effects of Air Plasma Species on Aqueous Solutes in Direct and Delayed Exposure Modes: Discharge, Post-Discharge and Plasma Activated Water," *Plasma Chemistry and Plasma Processing* 36 (2016): 355–381, https://doi.org/10.1007/s11090-015-9653-6.

80. P. Lukes, E. Dolezalova, I. Sisrova, and M. Clupek, "Aqueous-Phase Chemistry and Bactericidal Effects From an Air Discharge Plasma in Contact With Water: Evidence for the Formation of Peroxynitrite Through a Pseudo-Second-Order Post-Discharge Reaction of H_2O_2 and HNO_2," *Plasma Sources Science and Technology* 23 (2014): 015019, https://doi.org/10.1088/0963-0252/23/1/015019.

81. R. Zhou, R. Zhou, K. Prasad, et al., "Cold Atmospheric Plasma Activated Water as a Prospective Disinfectant: The Crucial Role of Peroxynitrite," *Green Chemistry* 20 (2018): 5276–5284, https://doi.org/10.1039/C8GC02800A.

82. S. Ikawa, A. Tani, Y. Nakashima, and K. Kitano, "Physicochemical Properties of Bactericidal Plasma-Treated Water," *Journal of Physics D: Applied Physics* 49 (2016): 425401, https://doi.org/10.1088/0022-3727/49/42/425401.

83. V. Veronico, P. Favia, F. Fracassi, R. Gristina, and E. Sardella, "The Active Role of Organic Molecules in the Formation of Long-Lived Reactive Oxygen and Nitrogen Species in Plasma-Treated Water Solutions," *Plasma Processes & Polymers* 19 (2022): e2100158, https://doi.org/10.1002/ppap.202100158.

84. F. Tampieri, Y. Gorbanev, and E. Sardella, "Plasma-Treated Liquids in Medicine: Let's Get Chemical," *Plasma Processes & Polymers* 20 (2023): e2300077, https://doi.org/10.1002/ppap.202300077.

85. A. Jaworek, A. M. Gañán-Calvo, and Z. Machala, "Low Temperature Plasmas and Electrosprays," *Journal of Physics D: Applied Physics* 52 (2019): 233001, https://doi.org/10.1088/1361-6463/ab0fdb.

86. J.-P. Borra, P. Ehouarn, and D. Boulaud, "Electrohydrodynamic Atomisation of Water Stabilised By Glow Discharge—Operating Range and Droplet Properties," *Journal of Aerosol Science* 35 (2004): 1313–1332, https://doi.org/10.1016/j.jaerosci.2004.05.011.

87. H.-H. Kim, J.-H. Kim, and A. Ogata, "Time-Resolved High-Speed Camera Observation of Electrospray," *Journal of Aerosol Science* 42 (2011): 249–263, https://doi.org/10.1016/j.jaerosci.2011.01.007.

88. B. Pongrác, H. H. Kim, M. Janda, V. Martišovitš, and Z. Machala, "Fast Imaging of Intermittent Electrospraying of Water With Positive Corona Discharge," *Journal of Physics D: Applied Physics* 47 (2014): 315202, https://doi.org/10.1088/0022-3727/47/31/315202.

89. M. Parhizkar, P. J. T. Reardon, J. C. Knowles, et al., "Performance of Novel High Throughput Multi Electrospray Systems for Forming of Polymeric Micro/Nanoparticles," *Materials & Design* 126 (2017): 73–84, https://doi.org/10.1016/j.matdes.2017.04.029.

90. A. Kleitz and J. M. Dorey, "Instrumentation for wet Steam," *Proceedings of the Institution of Mechanical Engineers, Part C: Journal of*

16128868, 0, Downloaded from https://onlinelibrary.wiley.com/doi/10.1002/ppap.202400275 by Mario Janda - Cochrane Slovakia , Wiley Online Library on [30/12/2024]. See the Terms and Conditions (https://onlinelibrary.wiley.com/terms-and-conditions) on Wiley Online Library for rules of use; OA articles are governed by the applicable Creative Commons License

Mechanical Engineering Science 218 (2004): 811–842, https://doi.org/10.1243/0954406041474192.

91. I. Bosdas, M. Mansour, A. I. Kalfas, and R. S. Abhari, "A Fast Response Miniature Probe for Wet Steam Flow Field Measurements," *Measurement Science and Technology* 27 (2016): 125901, https://doi.org/10.1088/0957-0233/27/12/125901.

92. X. Cai, D. Ning, J. Yu, et al., "Coarse Water in Low-Pressure Steam Turbines," *Proceedings of the Institution of Mechanical Engineers, Part A: Journal of Power and Energy* 228 (2014): 153–167, https://doi.org/10.1177/0957650913518767.

93. L. De Juan and J. F. De La Mora, "Charge and Size Distributions of Electrospray Drops," *Journal of Colloid and Interface Science* 186 (1997): 280–293, https://doi.org/10.1006/jcis.1996.4654.

94. K. Tang and A. Gomez, "Generation By Electrospray of Monodisperse Water Droplets for Targeted Drug Delivery By Inhalation," *Journal of Aerosol Science* 25 (1994): 1237–1249, https://doi.org/10.1016/0021-8502(94)90212-7.

95. M. Vazquez-Pufleau and P. M. Winkler, "Development of an Ultraviolet Constant Angle Mie Scattering Detector Toward the Determination of Aerosol Growth Kinetics in the Transition and Free Molecular Regime," *Aerosol Science and Technology* 54 (2020): 917–928, https://doi.org/10.1080/02786826.2020.1736504.

96. M. Janda, M. E. Hassan, V. Martišovitš, et al., "In Situ Monitoring of Electrosprayed Water Microdroplets Using Laser and LED Light Attenuation Technique: Comparison With Ultra-High-Speed Camera Imaging," *Journal of Applied Physics* 129 (2021): 183305, https://doi.org/10.1063/5.0046593.

97. D. Z. Pai, "Plasma-Liquid Interfacial Layer Detected By in Situ Raman Light Sheet Microspectroscopy," *Journal of Physics D: Applied Physics* 54 (2021): 355201, https://doi.org/10.1088/1361-6463/ac07e0.

98. K. Polprasarn, P. Pareek, D. Sadi, M. Janda, O. Guaitella, and D. Pai, "In Situ Raman Spectroscopy of Plasma Electrochemical and Plasma Catalytic Reactors," *ECS Meeting Abstracts* MA2024–01 (2024): 1408, https://doi.org/10.1149/MA2024-01241408mtgabs.

99. P. D. Maguire, C. M. O. Mahony, C. P. Kelsey, et al., "Controlled Microdroplet Transport in an Atmospheric Pressure Microplasma," *Applied Physics Letters* 106 (2015): 224101, https://doi.org/10.1063/1.4922034.

100. Z. Zhao, D. Liu, Y. Xia, et al., "The Dynamic Evolution of Atmospheric-Pressure Pulsed Air Discharge Over a Water Droplet," *Physics of Plasmas* 29 (2022): 043507, https://doi.org/10.1063/5.0083246.

101. Y. Chen, B. Peng, F. Qiu, et al., "Suspended Droplets Discharge Characteristics," *Plasma Processes & Polymers* (2024): e2400156, https://doi.org/10.1002/ppap.202400156.

102. N. Y. Babaeva, A. N. Bhoj, and M. J. Kushner, "Streamer Dynamics in Gases Containing Dust Particles," *Plasma Sources Science and Technology* 15 (2006): 591–602, https://doi.org/10.1088/0963-0252/15/4/001.

103. E. V. Sysolyatina, A. Y. Lavrikova, R. A. Loleyt, et al., "Bidirectional Mass Transfer-Based Generation of Plasma-Activated Water Mist With Antibacterial Properties," *Plasma Processes & Polymers* 17 (2020): 2000058, https://doi.org/10.1002/ppap.202000058.

104. J. De Oliveira Mallia, S. Griffin, C. Buttigieg, and R. Gatt, "A Rapid Prototyped Atmospheric Non-Thermal Plasma-Activated Aerosol Device and Anti-Bacterial Characterisation," *Frontiers in Chemistry* 12 (2024): 1416982, https://doi.org/10.3389/fchem.2024.1416982.

105. A. Upadrasta, S. Daniels, T. P. Thompson, B. Gilmore, and H. Humphreys, "In Situ Generation of Cold Atmospheric Plasma-Activated Mist and Its Biocidal Activity Against Surrogate Viruses for COVID-19," *Journal of Applied Microbiology* 134 (2023): lxad181, https://doi.org/10.1093/jambio/lxad181.

106. L. Guo, P. Zhao, Y. Jia, et al., "Inactivation of Airborne Pathogenic Microorganisms By Plasma-Activated Nebulized Mist," *Journal of Hazardous Materials* 459 (2023): 132072, https://doi.org/10.1016/j.jhazmat.2023.132072.

107. J. He, M. Waring, A. Fridman, et al., "Plasma-Generated Reactive Water Mist for Disinfection of N95 Respirators Laden With MS2 and T4 Bacteriophage Viruses," *Scientific Reports* 12 (2022): 19944, https://doi.org/10.1038/s41598-022-23660-5.

108. S. V. Belov, Y. K. Danileiko, S. V. Gudkov, et al., "A Device for Antibacterial Treatment of Hard Surfaces With Cold Mist Based on a Plasma-Activated Aqueous NaCl Solution," *Biomedical Engineering* 57 (2023): 153–158, https://doi.org/10.1007/s10527-023-10288-6.

109. I. Han, S. Mumtaz, and E. H. Choi, "Nonthermal Biocompatible Plasma Inactivation of Coronavirus SARS-CoV-2: Prospects for Future Antiviral Applications," *Viruses* 14 (2022): 2685, https://doi.org/10.3390/v14122685.

110. Y. Zhou, T. Jiang, L. Zhang, et al., "High Reactivity and Bactericidal Effects of Plasma-Activated Mist From Hydrogen Peroxide Solution," *Plasma Processes & Polymers* 20 (2023): 2200140, https://doi.org/10.1002/ppap.202200140.

111. Y. Song and X. Fan, "Cold Plasma Enhances the Efficacy of Aerosolized Hydrogen Peroxide in Reducing Populations of *Salmonella typhimurium* and *Listeria innocua* on Grape Tomatoes, Apples, Cantaloupe and Romaine Lettuce," *Food Microbiology* 87 (2020): 103391, https://doi.org/10.1016/j.fm.2019.103391.

112. J. Tan and M. V. Karwe, "Inactivation of *Enterobacter aerogenes* on the Surfaces of Fresh-Cut Purple Lettuce, Kale, and Baby Spinach Leaves Using Plasma Activated Mist (PAM)," *Innovative Food Science & Emerging Technologies* 74 (2021): 102868, https://doi.org/10.1016/j.ifset.2021.102868.

113. K. Hadinoto, H. Yang, T. Zhang, P. J. Cullen, S. Prescott, and F. J. Trujillo, "The Antimicrobial Effects of Mist Spraying and Immersion on Beef Samples With Plasma-Activated Water," *Meat Science* 200 (2023): 109165, https://doi.org/10.1016/j.meatsci.2023.109165.

114. H. Saadawy, E. M. Fathi, I. Elsayed, et al., "Treatment of Hepatocellular Carcinoma With in Situ Generated Plasma-Activated Air-Driven Water Mist," *Plasma Processes & Polymers* 20 (2023): e2200234, https://doi.org/10.1002/ppap.202200234.

115. J. R. Toth, N. H. Abuyazid, D. J. Lacks, J. N. Renner, and R. M. Sankaran, "A Plasma-Water Droplet Reactor for Process-Intensified, Continuous Nitrogen Fixation at Atmospheric Pressure," *ACS Sustainable Chemistry & Engineering* 8 (2020): 14845–14854, https://doi.org/10.1021/acssuschemeng.0c04432.

116. M. El Shaer, M. Abdel-azim, H. El-welily, et al., "Effects of DBD Direct Air Plasma and Gliding Arc Indirect Plasma Activated Mist on Germination, and Physiological Parameters of Rice Seed," *Plasma Chemistry and Plasma Processing* 43 (2023): 1169–1193, https://doi.org/10.1007/s11090-023-10350-x.

117. P. Škarpa, D. Klofáč, F. Krčma, J. Šimečková, and Z. Kozáková, "Effect of Plasma Activated Water Foliar Application on Selected Growth Parameters of Maize (*Zea mays* L.)," *Water* 12 (2020): 3545, https://doi.org/10.3390/w12123545.

118. S. Reuter, J. Winter, S. Iseni, et al., "The Influence of Feed Gas Humidity Versus Ambient Humidity on Atmospheric Pressure Plasma Jet-Effluent Chemistry and Skin Cell Viability," *IEEE Transactions on Plasma Science* 43 (2015): 3185–3192, https://doi.org/10.1109/TPS.2014.2361921.

119. G. Busco, F. Fasani, S. Dozias, et al., "Changes in Oxygen Level Upon Cold Plasma Treatments: Consequences for RONS Production," *IEEE Transactions on Radiation and Plasma Medical Sciences* 2 (2018): 147–152, https://doi.org/10.1109/TRPMS.2017.2775705.

120. R. Jangra, K. Ahlawat, M. K. Mohan, and R. Prakash, "Indoor Air Disinfection By Non Thermal Atmospheric Pressure Plasma: A Comparative Study of Performance in Low and High Humidity Environments," *Physica Scripta* 99 (2024): 085612, https://doi.org/10.1088/1402-4896/ad6353.

16128868, 0, Downloaded from https://onlinelibrary.wiley.com/doi/10.1002/ppap.202400275 by Mario Janda - Cochrane Slovakia , Wiley Online Library on [30/12/2024]. See the Terms and Conditions (https://onlinelibrary.wiley.com/terms-and-conditions) on Wiley Online Library for rules of use; OA articles are governed by the applicable Creative Commons License

121. D. A. Laroque, S. T. Seó, G. A. Valencia, J. B. Laurindo, and B. A. M. Carciofi, “Cold Plasma in Food Processing: Design, Mechanisms, and Application,” *Journal of Food Engineering* 312 (2022): 110748, https://doi.org/10.1016/j.jfoodeng.2021.110748.

122. M. Low, Y. M. Hung, and M. K. Tan, “Efficient Cooling of Light-Emitting Diode Via Plasma-Activated Aerosols,” *International Journal of Thermal Sciences* 206 (2024): 109313, https://doi.org/10.1016/j.ijthermalsci.2024.109313.

123. D. A. Saville, “Electrohydrodynamics: The Taylor-Melcher Leaky Dielectric Model,” *Annual Review of Fluid Mechanics* 29 (1997): 27–64, https://doi.org/10.1146/annurev.fluid.29.1.27.

124. A. Marchewicz, A. T. Sobczyk, A. Krupa, and A. Jaworek, “Induction Charging of Water Spray Produced By Pressure Atomizer,” *International Journal of Heat and Mass Transfer* 135 (2019): 631–648, https://doi.org/10.1016/j.ijheatmasstransfer.2019.02.013.

125. F. Di Natale, C. Carotenuto, L. D'Addio, et al., “Capture of Fine and Ultrafine Particles in a Wet Electrostatic Scrubber,” *Journal of Environmental Chemical Engineering* 3 (2015): 349–356, https://doi.org/10.1016/j.jece.2014.11.007.

126. L. Manna, F. Di Natale, C. Carotenuto, and A. Lancia, “Electrified Water Sprays Generation for Gas Pollutants Emission Control,” *Chemical Engineering Transactions* 52 (2016): 421–426, https://doi.org/10.3303/CET1652071.

127. Y. Higashiyama, S. Tanaka, T. Sugimoto, and K. Asano, “Size Distribution of the Charged Droplets in an Axisymmetric Shower,” *Journal of Electrostatics* 47 (1999): 183–195, https://doi.org/10.1016/S0304-3886(99)00042-X.

128. G. Castle and I. Inculet, “Induction Charge Limits of Small WAter Droplets," in *The Eighth International Conference on Electrostatics* (10–12, April 1991, England: Oxford, 1991), 141–146.

129. L. Manna, “Characterization of Electrified Water Sprays” (Ph.D. Thesis, University of Naples Federico II, 2018).

130. L. P. Di Bonito, A. Parisi, and F. Di Natale, "Electrohydrodynamic Atomisation of Water From a Hydraulic Flat Fan Spray Nozzle” (Sixth European Symposium on Electrohydrodynamic Atomization and Electrospinning (Kraków, Poland, 10–12 May, 2023, 2023).

131. S. Kooshki, P. Pareek, M. Janda, and Z. Machala, “Selective Reactive Oxygen and Nitrogen Species Production in Plasma-Activated Water Via Dielectric Barrier Discharge Reactor: An Innovative Method for Tuning and Its Impact on Dye Degradation,” *Journal of Water Process Engineering* 63 (2024): 105477, https://doi.org/10.1016/j.jwpe.2024.105477.

132. J. Fujera, T. Homola, V. Jirásek, et al., “Aerosol-Based Multihollow Surface Dbd: A Promising Approach for Nitrogen Fixation,” *Plasma Sources Science and Technology* 33 (2024): 075002, https://doi.org/10.1088/1361-6595/ad590b.

133. S. Wang, J. Wang, C. Song, and J. Wen, “Numerical Investigation on Urea Particle Removal in a Spray Scrubber Using Particle Capture Theory,” *Chemical Engineering Research and Design* 145 (2019): 150–158, https://doi.org/10.1016/j.cherd.2019.03.011.

134. H. Zhang, G. Huang, C. Gong, Y. Yang, and Y. Pan, “Corona Discharge-Induced Water Droplet Growth in Air,” *IEEE Transactions on Plasma Science* 48 (2020): 2437–2441, https://doi.org/10.1109/TPS.2020.2999912.

135. G. Nayak, M. Meyer, G. Oinuma, M. J Kushner, and P. J Bruggeman, “The Transport Dynamics of Tens of Micrometer-Sized Water Droplets in RF Atmospheric Pressure Glow Discharges,” *Plasma Sources Science and Technology* 32 (2023): 045005, https://doi.org/10.1088/1361-6595/acc54a.

136. K. K. Moß, K.-G. Reinsberg, and J. A. C. Broekaert, “Study of a Direct Current Atmospheric Pressure Glow Discharge in Helium With Wet Aerosol Sample Introduction Systems,” *Journal of Analytical Atomic Spectrometry* 29 (2014): 674, https://doi.org/10.1039/c3ja50190f.

137. D. Aceto, P. R. Rotondo, M. Ambrico, et al., "Atmospheric Pressure, Low Temperature Plasma Applications for Decontamination of Agri-food Products" (ESCAMPIG XXVI, Brno, Czech Republic, July 9–13, 2024).

16128868, 0, Downloaded from https://onlinelibrary.wiley.com/doi/10.1002/ppap.202400275 by Mario Janda - Cochrane Slovakia , Wiley Online Library on [30/12/2024]. See the Terms and Conditions (https://onlinelibrary.wiley.com/terms-and-conditions) on Wiley Online Library for rules of use; OA articles are governed by the applicable Creative Commons License